

1

2 **Investigating water budget dynamics in 18 river basins across**  
3 **Tibetan Plateau through multiple datasets**

4 Wenbin Liu<sup>a</sup>, Fubao Sun<sup>a,b,h,i,\*</sup>, Yanzhong Li<sup>c</sup>, Guoqing Zhang<sup>d,e</sup>, Yan-Fang Sang<sup>a</sup>,  
5 Wee Ho Lim<sup>a,f</sup>, Jiahong Liu<sup>g</sup>, Hong Wang<sup>a</sup>, Peng Bai<sup>a</sup>

6

7 <sup>a</sup> Key Laboratory of Water Cycle and Related Land Surface Processes, Institute of Geographic  
8 Sciences and Natural Resources Research, Chinese Academy of Sciences, Beijing 100101, China

9 <sup>b</sup> Hexi University, Zhangye 734000, China

10 <sup>c</sup> College of Hydrometeorology, Nanjing University of Information Science and Technology,  
11 Nanjing 210044, China

12 <sup>d</sup> Key Laboratory of Tibetan Environmental Changes and Land Surface Processes, Institute of  
13 Tibetan Plateau Research, Chinese Academy of Sciences, Beijing 100101, China

14 <sup>e</sup> CAS Center for Excellent in Tibetan Plateau Earth Sciences, Beijing 100101, China

15 <sup>f</sup> Environmental Change Institute, Oxford University Centre for the Environment, School of  
16 Geography and the Environment, University of Oxford, Oxford OX1 3QY, UK

17 <sup>g</sup> Key Laboratory of Simulation and Regulation of Water Cycle in River Basin, China Institute of  
18 Water Resources and Hydropower Research, Beijing 100038, China

19 <sup>h</sup> College of Resources and Environment, University of Chinese Academy of Sciences, Beijing  
20 100049, China

21 <sup>i</sup> Center for Water Resources Research, Chinese Academy of Sciences, Beijing 100101, China

22

23 **Re-submitted to:** Hydrology and Earth System Sciences

24 **Corresponding Author:** Dr. Fubao Sun ([Sunfb@igsnr.ac.cn](mailto:Sunfb@igsnr.ac.cn)), Key Laboratory of Water Cycle  
25 and Related Land Surface Processes, Institute of Geographic Sciences and Natural Resources  
26 Research, Chinese Academy of Sciences

27 2017/11

28 **Abstract** The dynamics of basin-scale water budgets are not well understood  
29 nowadays over the Tibetan Plateau (TP) due to the lack of in situ hydro-climatic  
30 observations. In this study, we investigate the seasonal cycles and trends of water  
31 budget components (e.g., precipitation-P, evapotranspiration-ET and runoff-Q) in  
32 eighteen TP river basins during the period 1982-2011 through the use of multi-source  
33 datasets (e.g., in situ observations, satellite retrievals, reanalysis outputs and land  
34 surface model simulations). A water balance-based two-step procedure, which  
35 considers the changes in basin-scale water storage at the annual scale, is also adopted  
36 to calculate actual ET. The results indicated that precipitation (mainly snowfall from  
37 mid-autumn to next spring), which mainly concentrated during June-October (varied  
38 among different monsoons-impacted basins), was the major contributor to the runoff  
39 in TP basins. The P, ET and Q were found marginally increase in most TP basins  
40 during the past 30 years except for the upper Yellow River basin and some sub-basins  
41 of Yalong River, which were mainly affected by the weakening East Asian Monsoon.  
42 Moreover, the aridity index ( $PET/P$ ) and runoff coefficient ( $Q/P$ ) slightly decreased in  
43 most basins, which were in agreement with the warming and moistening climate in  
44 the Tibetan Plateau. The results obtained demonstrated the usefulness of integrating  
45 multi-source datasets to hydrological applications in the data-sparse regions. More  
46 generally, such approach might offer helpful insights towards understanding the water  
47 and energy budgets and sustainability of water resource management practices of  
48 data-sparse regions in a changing environment.

49

## 50 **1 Introduction**

51 As the highest plateau in the globe (the average elevation is higher than 4000 meters  
52 above the sea level), the Tibetan Plateau (TP, also called “the roof of the world” or  
53 “the third Pole”) is regarded as one of the most vulnerable regions under a warming  
54 climate and is exposed to strong interactions among atmosphere, hydrosphere,  
55 biosphere and cryosphere in the earth system (Duan and Wu, 2006; Yao et al., 2012;  
56 Liu et al., 2016b). It also serves as the “Asian water tower” from which some major  
57 Asian rivers such as Yellow River, Yangtze River, Brahmaputra River, Mekong River,  
58 Indus River, etc., originate, which is a vital water resource to support the livelihood of  
59 hundreds of millions of people in China and the neighboring Asian countries  
60 (Immerzeel et al., 2010; Zhang et al., 2013). Hence sound knowledge of water budget  
61 and hydrological regimes in TP river basins and their responses to the changing  
62 environment would have practical relevance for achieving sustainable water resource  
63 management and environmental protection in this part of the world (Yang et al., 2014;  
64 Chen et al., 2015).

65  
66 Despite the importance of TP in this geographic region, advance in hydrological and  
67 land surfaces studies in this region has been limited by data scarcity (Zhang et al.,  
68 2007; Li F. et al., 2013; Liu X. et al., 2016). For instance, less than 80 observation  
69 stations (~10% of a total of ~750 observation station across China) have been  
70 established in TP by the Chinese Meteorological Administration (CMA) since the  
71 mid-20<sup>th</sup> century (Wang and Zeng, 2012). These stations are generally sparse and  
72 unevenly distributed at relatively low elevation regions (most stations are located in  
73 the eastern TP and few of them situated in the western parts), focus only on the  
74 meteorological variables and lack of other land surface observations such as

75 evapotranspiration, snow water equivalent and latent heat fluxes. In addition,  
76 long-term observations of river discharge, lake depth and glacier melts in the TP are  
77 also absent (Akhta et al., 2009; Ma et al., 2016). Therefore, the water budget and  
78 hydrological regimes for each river basin of TP and their relation with atmospheric  
79 circulations are poorly understood (Cuo et al., 2014; Xu et al., 2016). Whilst this  
80 shortcoming could be resolved through installation of in-situ monitoring systems  
81 (Yang et al., 2013; Zhou et al., 2013; Ma et al., 2015), the overall cost, labor and  
82 technical support for running the operational sites would be substantial. Another  
83 workaround would be through modeling approach, i.e., feeding remote sensing  
84 information and meteorological forcing data into physically-based land surface model  
85 (LSM) to simulate the basin-wide water budget (Bookhagen and Burbank, 2010; Xue  
86 et al., 2013; Zhang et al., 2013; Cuo et al., 2015; Zhou et al., 2015; Wang et al., 2016).  
87 However, such approach is not immune from the issue of data scarcity at multiple  
88 river basins (with varied sizes and/or terrain complexities) for supporting model  
89 calibration and validation purposes (Li F. et al., 2014).

90

91 Most recently, several global (or regional) datasets relevant to the calculation of water  
92 budget have been released. They include remote sensing-based retrievals (Tapley et al.,  
93 2004; Zhang et al., 2010; Long et al., 2014; Zhang Y. et al., 2016), land surface model  
94 (LSM) simulations (Rui, 2011), reanalysis outputs (Berrisford et al., 2011; Kobayashi  
95 et al., 2015) and gridded forcing data interpolated from the in situ observations  
96 (Harris et al., 2014). For example, there are many products related to terrestrial  
97 evapotranspiration (ET) such as GLEAM\_E (Global Land surface Evaporation: the  
98 Amsterdam Methodology, Miralles et al., 2011a), MTE\_E (a product integrated the  
99 point-wise ET observation at FLUXNET sites with geospatial information extracted

100 from surface meteorological observations and remote sensing in a machine-learning  
101 algorithm, Jung et al., 2010 ), LSM-simulated ETs from Global Land Data  
102 Assimilation System version 2 (GLDAS-2) with different land surface schemes  
103 (Rodell et al., 2004), ETs from Japanese 55-year reanalysis (JRA55\_E), the  
104 ERA-Interim global atmospheric reanalysis dataset (ERA-Interim) and the National  
105 Aeronautic and Space Administration (NASA) Modern Era Retrospective-analysis  
106 for Research and Application (MERRA) reanalysis data (Lucchesi, 2012). Moreover,  
107 there are also several global or regional LSM-based runoff simulations from GLDAS  
108 and the Variable Infiltration Capacity (VIC) model (Zhang et al., 2014). A few  
109 attempts have been made to validate multiple datasets for certain water budget  
110 components and to explore their possible hydrological implications. For example, Li  
111 X. et al. (2014) and Liu et al. (2016a) evaluated multiple ET estimates against the  
112 water balance method at annual and monthly time scales. Bai et al. (2016) assessed  
113 streamflow simulations of GLDAS LSMs in five major rivers over the TP based on  
114 the discharge observations. Although uncertainties might exist among different  
115 datasets with various spatial and temporal resolutions and calculated using different  
116 algorithms (Xia et al., 2012), they offer an opportunity to examine the general  
117 basin-wide water budgets and their uncertainties in gauge-sparse regions such as the  
118 TP considered in this study.

119

120 From the multiple datasets perspective, this study aims to investigate the water budget  
121 in 18 TP river basins distributed across the Tibetan Plateau; and evaluate seasonal  
122 cycles and annual trends of these water budget components. This paper is organized  
123 as follows: the datasets and methods applied in this study are described in Sect.2. The  
124 results of season cycles and annual trends of water budget components for the river

125 basins are presented and discussed in Sect.3. The uncertainties arise from employing  
126 multiple datasets are also discussed in the same section. In Sect.4, we generalize our  
127 findings which would be helpful for understanding the water balances of the river  
128 basins under constant influence of interplay between westerlies and monsoons (e.g.,  
129 Indian monsoon, East Asian monsoon) in the Tibetan Plateau.

130

## 131 **2 Data and methods**

### 132 **2.1 Multiple datasets used**

#### 133 **2.1.1 Runoff, precipitation and terrestrial storage change**

134 We obtained the observed daily runoff (Q) during the period 1982-2011 from the  
135 National Hydrology Almanac of China (Table 1). There are < 30% missing data in  
136 some gauging stations such as Yajiang, Tongren, Gandatan and Zelingou. Therefore,  
137 the VIC Retrospective Land Surface Dataset over China (1952-2012, VIC\_IGSNRR  
138 simulated) with a spatial resolution of 0.25 degree and a daily temporal resolution  
139 from the Geographic Sciences and Natural Resources Research (IGSNRR), Chinese  
140 Academy of Sciences, is also used. This dataset is derived from the VIC model forced  
141 by the gridded daily observed meteorological forcing (IGSNRR\_forcing) (Zhang et al.,  
142 2014). A degree-day scheme was used in the model to account for the influences of  
143 snow and glacier on hydrological processes.

144

145 In terms of precipitation (P), we used the gridded monthly precipitation dataset  
146 available at CMA (spatial resolution of 0.5 degree; 1961-2011; interpolated from  
147 observations of 2372 national meteorological stations using the Thin Plate Spline  
148 method) (Table 1). Since the reliability of this dataset might be restricted by the  
149 relatively sparse stations and complex terrain conditions of TP, we make an attempt to

150 incorporate two other precipitation datasets ((IGSNRR\_forcing and Tropical Rainfall  
151 Measuring Mission TRMM 3B43 V7). The precipitation from IGSNRR forcing  
152 datasets (0.25 degree) was derived by interpolating gauged daily precipitation from  
153 756 CMA stations based on the synergraphic mapping system algorithm (Shepard,  
154 1984; Zhang et al., 2014) and was further bias-corrected using the CMA gridded  
155 precipitation.

156 <Table 1, here please, thanks>

157 To get the change in terrestrial storage ( $\Delta S$ ), we used three latest global terrestrial  
158 water storage anomaly and water storage change datasets (available on the GRACE  
159 Tellus website: <http://grace.jpl.nasa.gov/>) that were retrieved from the Gravity  
160 Recovery and Climate Experiment (GRACE, Tapley et al., 2004; Landerer and  
161 Swenson, 2012; Long et al., 2014). Briefly, they were processed separately at the Jet  
162 Propulsion Laboratory (JPL), the GeoForschungsZentrum (GFZ) and the Center for  
163 Space Research at the University of Texas (CSR). To minimize the errors and  
164 uncertainty of extracted  $\Delta S$ , we averaged these GRACE retrievals (2002-2013) from  
165 different processing centers in this study.

166

### 167 **2.1.2 Temperature, potential evaporation and ET**

168 We obtained the monthly gridded temperature dataset (0.5 degree) from CMA; and  
169 potential evaporation (PET) dataset (0.5 degree, Harris et al., 2013) from Climatic  
170 Research Unit (CRU), University of East Anglia. Moreover, we used six global  
171 /regional ET products (four diagnostic products and two LSMs simulations, Table 1),  
172 namely (1) GLEAM\_E (Miralles et al., 2010, 2011), which consists of three sources  
173 of ET (transpiration, soil evaporation and interception) for bare soil, short vegetation

174 and vegetation with a tall canopy calculated using a set of algorithm ([www.gleam.eu](http://www.gleam.eu)),  
175 (2) GNoah\_E simulated using GLDAS-2 with the Catchment Noah scheme  
176 (<http://disc.sci.gsfc.nasa.gov/hydrology/data-holdings>) (Rodell et al., 2004), (3)  
177 Zhang\_E (Zhang et al., 2010), which is estimated using the modified  
178 Penman-Monteith equation forced with MODIS data, satellite-based vegetation  
179 parameters and meteorological observations (<http://www.ntsg.umd.edu/project/et>), (4)  
180 MET\_E (Jung et al., 2010) (<https://www.bgc-jena.mpg.de/geodb/projects/Home.phs>),  
181 (5) VIC\_E (Zhang et al., 2014) from VIC\_IGSNRR simulations  
182 ([http://hydro.igsnrr.ac.cn/public/vic\\_outputs.html](http://hydro.igsnrr.ac.cn/public/vic_outputs.html)) and (6) PML\_E (Zhang Y. et al.,  
183 2016) computed from global observation-driven Penman-Monteith-Leuning (PML)  
184 model (<https://data.csiro.au/dap/landingpage?pid=csiro:17375&v=2&d=true>).  
185

### 186 **2.1.3 Vegetation and snow/glacier parameters**

187 To quantify the dynamics of vegetation of each river basin, we applied the  
188 Normalized Difference Vegetation Index (NDVI) and the Leaf Area Index (LAI)  
189 (Table 1). Briefly, the NDVI data was obtained from the Global Inventory Modeling  
190 and Mapping Studies (GIMMS) (Turker et al., 2005)  
191 ([https://nex.nasa.gov/nex/projects/1349/wiki/general\\_data\\_description\\_and\\_access/](https://nex.nasa.gov/nex/projects/1349/wiki/general_data_description_and_access/))  
192 while the LAI data was collected from the Global Land Surface Satellite (GLASS)  
193 products (<http://www.glcf.umd.edu/data/lai/>) (Liang and Xiao, 2012). Whist the  
194 change in seasonal snow cover and glacier has significant impact on the water and  
195 energy budgets in TP river basins; it remains a technical challenge to get reliable  
196 observations due to harsh environment (especially at the basin scale). However,  
197 recently available satellite-based/LSM-simulated products might provide adequate



198 characterization of the variation of snow cover and glacier. To quantify the change in  
199 snow cover at each basin, we applied the daily cloud free snow composite product  
200 from MODIS Terra-Aqua and the Interactive Multisensor Snow and Ice Mapping  
201 System for the Tibetan Plateau (Zhang et al., 2012; Yu et al., 2015), in conjunction  
202 with the snow water equivalent (SWE) retrieved from Global Snow Monitoring for  
203 Climate Research product (GlobSnow-2, <http://www.globsnow.info/>) and the  
204 VIC\_IGSNRR simulations (Takala et al., 2011; Zhang et al., 2014). We extracted  
205 general distribution of glacier of TP from the Second Glacier Inventory Dataset of  
206 China (Guo et al., 2014). All gridded datasets used were first uniformly interpolated to  
207 a spatial resolution of 0.5 degree based on the bilinear interpolation to make their  
208 inter-comparison possible. The datasets were then extracted for each of TP basins.

209

#### 210 **2.1.4 Monsoon indices**

211 In general, the TP climate is under the influences of the westerlies, Indian summer  
212 monsoon and East Asian summer monsoon (Yao et al., 2012). To investigate the  
213 changes of monsoon systems and their potential impacts on water budgets in the TP  
214 basins, we used three monsoon indices, namely Asian Zonal Circulation Index (AZCI),  
215 Indian Ocean Dipole Mode Index (IODMI) and East Asian Summer Monsoon Index  
216 (EASMI). Briefly, the IODMI (reflects the dynamics of Indian Summer Monsoon) is  
217 an indicator of the east-west temperature gradient across the tropical Indian Ocean  
218 (Saji et al., 1999), which can be downloaded from the following website:  
219 [http://www.jamstec.go.jp/frcgc/research/d1/iod/HTML/Dipole%20Mode%20Index.ht](http://www.jamstec.go.jp/frcgc/research/d1/iod/HTML/Dipole%20Mode%20Index.html)  
220 [ml](http://www.jamstec.go.jp/frcgc/research/d1/iod/HTML/Dipole%20Mode%20Index.html). The EASMI and AZCI (60°-150°E) reflect the dynamics of East Asian summer  
221 monsoon (Li and Zeng, 2002) and the westerlies (represented by Asian Zonal  
222 Circulation index), which can be obtained from Beijing Normal University

223 (<http://ljp.gcess.cn/dct/page/65577>) and the National Climate Center of China  
224 (<http://ncc.cma.gov.cn/Website/index.php?ChannelID=43WCHID=5>), respectively.

225

### 226 **2.1.5 Study basins**

227 In this study, we selected 18 river basins of varied sizes (range: 2832-191235 km<sup>2</sup> ;  
228 see Table 2 for details) with adequate runoff data over a 30-year period (1982-2011).  
229 They are distributed in the northwestern, southeastern and eastern parts of the plateau  
230 with multiyear-mean and basin-averaged temperature and precipitation ranging from  
231 -5.68 to 0.97 °C and 128 to 717 mm, which are solely dominated or under the  
232 combined influences of the westerlies, the Indian Summer monsoon and the East  
233 Asian monsoon (Yao et al., 2012). There are more glacier and snow covers in the  
234 westerlies-dominant basins such as Yerqiang, Yulongkashi and Keliya (10.86-23.27%  
235 and 29.16-35.95%, respectively); less for the East Asian monsoon-dominated basins  
236 such as Yellow, Yangtze and Bayin (0-0.96% and 9.42-20.05%, respectively) (Table  
237 2).

238 <Figure 1, here please, thanks>

239 <Table 2, here please, thanks>

240

## 241 **2.2 Methods**

### 242 **2.2.1 Water balance-based ET estimation**

243 The basin-wide water balance at the monthly and annual timescales could be written  
244 as the principle of mass conservation (also known as the continuity equation, Oliveira  
245 et al., 2014) of basin-wide precipitation (P, mm), evapotranspiration (ET<sub>wb</sub>, mm),  
246 runoff (Q, mm) as well as terrestrial water storage change (ΔS, mm),

$$247 \quad ET_{wb} = P - Q - \Delta S \quad (1)$$

248 The terrestrial water storage ( $\Delta S$ ) in Eq. (1) includes the surface, subsurface and  
249 ground water changes. It has been demonstrated that  $\Delta S$  cannot be neglected in water  
250 balance calculation over monthly and annual timescales due to snow cover change  
251 and anthropogenic interferences (e.g., reservoir operation, agricultural water  
252 withdrawal) (Liu et al., 2016a). For the period 2002-2011, we calculated basin-wide  
253 ET ( $ET_{wb}$ ) directly using the GRACE-derived  $\Delta S$  in Eq. (1). Since GRACE data is  
254 absent before 2002, we calculated the monthly  $ET_{wb}$  using the following two-step  
255 bias-correction procedure (Li X. et al., 2014). We defined  $P - Q$  in Eq. (1) as biased  
256 ET ( $ET_{biased}$ , available from 1982 to 2011) relative to the “true” ET ( $ET_{wb} = P - Q -$   
257  $\Delta S$ , available during the period 2002-2011 when the GRACE data is available). Over  
258 the period 2002-2011, we first fitted  $ET_{biased}$  and  $ET_{wb}$  series separately using  
259 different gamma distributions, which has been evidenced as an proper method for  
260 modeling the probability distribution of ET (Bouraoui et al., 1999). The monthly  
261  $ET_{biased}$  series (2002-2011) can then be bias-corrected through the inverse function  
262 ( $F^{-1}$ ) of the gamma cumulative distribution function (CDF,  $F$ ) of  $ET_{wb}$  by matching  
263 the cumulative probabilities between two CDFs as follow (Liu et al., 2016a),

$$264 \quad ET_{corrected}(m) = F^{-1}(F(ET_{biased}(m)|\alpha_{biased}, \beta_{biased})|\alpha_{wb}, \beta_{wb}) \quad (2)$$

265 Here  $\alpha_{biased}, \beta_{biased}$  and  $\alpha_{wb}, \beta_{wb}$  are shape and scale parameters of  
266 gamma distributions for  $ET_{biased}$  and  $ET_{wb}$ .  $ET_{corrected}(m)$  and  $ET_{biased}(m)$   
267 represent the monthly corrected and biased ET, respectively. The bias correction  
268 procedure can be flexibly applied to the period 1983-2011 by matching the CDF  
269 of  $ET_{biased}$  (1983-2011) to that of  $ET_{corrected}$  (2002-2011). The second step of  
270 bias correction is to eliminate the annual bias through the ratio of annual  
271  $ET_{biased}$  to annual  $ET_{corrected}$  calculated in the first step using the following  
272 method,

273 
$$ET_{\text{final}}(m) = \frac{ET_{\text{biased}}(a)}{ET_{\text{corrected}}(a)} \times ET_{\text{corrected}}(m) \quad (3)$$

274 where  $ET_{\text{final}}(m)$  is the final monthly ET after bias correction.  $ET_{\text{biased}}(a)$  and  
 275  $ET_{\text{corrected}}(a)$  represent the annual biased and corrected ET while  
 276  $ET_{\text{corrected}}(m)$  is the monthly corrected ET obtained from the first step. The  
 277 procedure was then applied to correct the monthly  $ET_{\text{biased}}$  series and  
 278 calculated the monthly  $ET_{\text{corrected}}$  during the period 1982-2001 for all TP  
 279 basins. We take these results as sufficient representation of the “true” ET ( $ET_{\text{wb}}$ )  
 280 for evaluating multiple ET products and trend analysis. ”

281

### 282 **2.2.2 Modified Mann-Kendall test method**

283 The Mann-Kendall (MK) test is a rank-based nonparametric approach which is less  
 284 sensitive to outlier relative to other parametric statistics, but it is sometimes  
 285 influenced by the serial correlation of time series. Pre-whitening is often used to  
 286 eliminate the influence of lag-1 autocorrelation before the use of MK test. For  
 287 example,  $X(X_1, X_2, \dots, X_n)$  is a time series data, it will be replaced by  $(X_2 -$   
 288  $cX_1, X_3 - cX_2, \dots, X_{n+1} - cX_n)$  in pre-whitening if the lag-1 autocorrelation  
 289 coefficient ( $c$ ) is larger than 0.1 (von Storch, 1995). However, significant lag- $i$   
 290 autocorrelation may still be detected after pre-whitening because only the lag-1  
 291 autocorrelation is considered in pre-whitening (Zhang et al., 2013). Moreover, it  
 292 sometimes underestimate the trend for a given time series (Yue et al., 2002). Hamed  
 293 and Rao (1998) proposed a modified version of MK test (MMK) to consider the lag- $i$   
 294 autocorrelation and related robustness of the autocorrelation through the use of  
 295 equivalent sample size, which has been widely used in previous studies during the last  
 296 five decades (McVicar et al., 2012; Zhang et al., 2013; Liu and Sun, 2016). In the  
 297 MMK approach, if the lag- $i$  autocorrelation coefficients are significantly distinct from

298 zero, the original variance of MK statistics will be replaced by the modified one. In  
299 this study, we used the MMK approach to quantify the trends of water budget  
300 components in 18 TP basins and the significance of trend was tested at the >95%  
301 confidence level.

302

### 303 **3 Results and Discussion**

#### 304 **3.1 ET evaluation and General hydrological characteristics of 18 TP basins**

305 We first assessed the VIC\_IGSNRR simulated runoff against the observations for  
306 each basin (for example, at Tangnaihahi and Pangduo stations in Fig.2). If the Nash  
307 Efficiency coefficient (NSE) between the observation and simulation is above 0.65,  
308 the VIC\_IGSNRR simulated runoff is acceptable and could be used to replace the  
309 missing runoff values for a given basin. Moreover, the CMA precipitation is  
310 consistent with TRMM (Corr = 0.86, RMSE = 8.34 mm/month) and IGSNRR forcing  
311 (Corr = 0.94, RMSE = 7.15mm/month) precipitation for multiple basins (i.e., for the  
312 smallest basin above Tongren station, Fig.2). Moreover, the magnitudes of  
313 GRACE-derived annual mean water storage change ( $\Delta S$ ) in 18 TP basins are  
314 relatively less than those for other water balance components such as annual P, Q and  
315 ET (Table 2 and Table 3). The uncertainties among GRACE-derived annual mean  $\Delta S$   
316 from different data processing centers (CSR, GFZ and JPL) are small for 18 basins  
317 except for the basins controlled by Gadatan and Tangnaihahi stations.

318 < Figure 2, here please, thanks >

319 < Table 3, here please, thanks >

320 We then evaluated six ET products in 18 TP basins against our calculated  $ET_{wb}$  at a  
321 monthly basis during the period 1983-2006 (Fig. 3). The ranges of monthly averaged  
322 ET among different basins (approximately 4–39 mm/month) are very close for all

323 products compare to that calculated from the  $ET_{wb}(6-42 \text{ mm/month})$ . However,  
324 GLEAM\_E (correlation coefficient:  $\text{Corr} = 0.85$  and root-mean-square-error:  $\text{RMSE} =$   
325  $5.69 \text{ mm/month}$ ) and VIC\_E ( $\text{Corr} = 0.82$  and  $\text{RMSE} = 6.16 \text{ mm/month}$ ) perform  
326 relatively better than others. Although Zhang\_E and GNoah\_E were found closely  
327 correlated to monthly  $ET_{wb}$  in the upper Yellow River, the upper Yangtze River,  
328 Qiangtang and Qaidam basins (Li X. et al., 2014), they did not exhibit overall good  
329 performances ( $\text{Corr} = 0.61$ ,  $\text{RMSE} = 7.97 \text{ mm/month}$  for Zhang\_E and  $\text{Corr} = 0.42$ ,  
330  $\text{RMSE} = 10.16 \text{ mm/month}$  for GNoah\_E) for 18 TP basin used in this study. We thus  
331 use GLEAM\_E and VIC\_E together with  $ET_{wb}$  to analyze the seasonal cycles and  
332 trends of ET in 18 TP basins in the following sections.

333 < Figure 3, here please, thanks >

334 To investigate the general hydroclimatic characteristics of river basins over the TP, we  
335 classify 18 basins into three categories, namely westerlies-dominated basins  
336 (Yerqiang, Yulongkashi and Kelia), Indian monsoon-dominated basins (Brahmaputra  
337 and Salween), and East Asian monsoon-dominated basins (Yellow, Yalong and  
338 Yangtze) referred to Tian et al. (2007), Yao et al. (2012) and Dong et al. (2016).  
339 Interestingly, they are clustered into three groups under Budyko framework (Budyko,  
340 1974; Zhang D. et al., 2016) with relatively lower evaporative index in Indian  
341 monsoon-dominant basins and higher aridity index in westerlies-dominant basins,  
342 which reveal various long-term hydroclimatologic conditions (Fig. 4). Overall, from  
343 the westerlies-dominant, Indian monsoon-dominant to East Asian monsoon-dominant  
344 basins, the annual mean air temperature ( $-5.68$  -  $-0.97 \text{ }^\circ\text{C}$ ) and ET (and thus runoff  
345 coefficient gradually decreases) increases while the multiyear mean glacier area (and  
346 thus the glacier melt normalized by precipitation) gradually decreases (Fig. 4 and  
347 Table 2). Moreover, the vegetation status (NDVI range: 0.05-0.43; LAI range:

348 0.03-0.83) tends to be better. The  $R^2$  between basin-averaged NDVI and ET (0.76) is  
349 much higher than that between T and NDVI (0.35), which indicating that the water  
350 availability plays a more important role than the heat stress (i.e., colder status) over  
351 such basins. The results are in line with Shen et al. (2015), which indicated that the  
352 spatial pattern of ET trend was significantly and positively correlated with NDVI  
353 trend over the TP. The dominant climate systems are overall discrepant for the three  
354 TP regions with different water-energy characteristics and sources of water vapor. For  
355 example, in the westerlies-controlled basins, more glaciers developed due to their  
356 relatively colder air temperature and special seasonality of precipitation. Therefore,  
357 there are more snow melt contributions to total river streamflow with global warming  
358 during the period 1983-2006. It is a general picture of hydrological regime in  
359 high-altitude and cold regions (Zhang et al., 2013; Cuo et al., 2014), which could be  
360 interpreted from the perspective of multi-source datasets in the data-sparse TP.

361 < Figure 4, here please, thanks >

### 362 **3.2 Seasonal cycles of basin-wide water budget components for the TP basins**

363 The multi-year means of water budget components (i.e., P, Q, ET, snow cover and  
364 SWE) and vegetation parameters (i.e., NDVI and LAI) are calculated for each  
365 calendar month and for 18 TP river basins using multi-source datasets available from  
366 1982 to 2011. Overall, the seasonal variations of P, Q, ET, air temperature and  
367 vegetation parameters are similar in all TP basins with peak values occurred in May to  
368 September (Fig.5 and Fig.6). The seasonal cycles of snow cover and SWE are  
369 generally consistent among the basins (the peak values mainly occur from October to  
370 next April, Fig.7). With the ascending air temperature from cold to warm months, the  
371 basin-wide precipitation increases and vegetation cover expands gradually (the  
372 basin-wide ET also increase). Meanwhile, snow cover and glaciers retreat gradually

373 with the melt water supplying the river discharge together with precipitation. The  
374 inter-basin variations of hydrological regime are to a large extent linked to the climate  
375 systems that prevail over the TP.

376 < Figure 5, here please, thanks >

377 Although the temporal patterns of hydrological components are generally analogous,  
378 they vary among the parameters, climate zones and even basins (Zhou et al., 2005).  
379 For example, relative to air temperature, the seasonal pattern of runoff is similar to  
380 precipitation which reveals that runoff is mainly controlled by precipitation in most  
381 TP basins. It is in agreement with that summarized by Cuo et al. (2014). In the  
382 westerlies-dominated basins, the peak values of precipitation and runoff mainly  
383 concentrate in June-August, which contribute approximately 68-82% and 67-78% of  
384 annual totals, respectively. During this period, the runoff always exceeds precipitation  
385 which indicates large contributions of glacier/snow-melt water to streamflow. It is  
386 consistent with the existing findings in Tarim River (Yerqiang, Yulongkashi and  
387 Keliya rivers are the major tributaries of Tarim River), which indicated that the melt  
388 water accounted for about half of the annual total streamflow (Fu et al., 2008). The  
389 ET (vegetation cover) in three westerlies-dominated basins are relatively less (scarcer)  
390 than that in other TP basins while the percentages of glacier and seasonal snow cover  
391 are higher in these basins which contribute more melt water to river discharge (Fig.6  
392 and Fig.7). Overall, the SWE in Yerqiang, Yulongkashi and Keliya rivers are higher in  
393 winter than other seasons, but they vary with basins and products which reflect  
394 considerable uncertainties in SWE estimations.

395 < Figure 6, here please, thanks >

396 In the Indian monsoon and East Asian monsoon dominated basins, the runoff  
397 concentrates during June-September (or June- October) with precipitation being the



398 dominant contributor of annual total runoff. For example, the peak values of  
399 precipitation and runoff occur during June-September at Zhimenda station  
400 (contributing about 80% and 74% of the annual totals) while those occur during  
401 June-October at Tangnaihai station (contributing about 78% and 71% of the annual  
402 totals, respectively). The results are quite similar to the related studies in eastern and  
403 southern TP such as Liu (1999), Dong et al. (2007), Zhu et al. (2011), Zhang et al.  
404 (2013), Cuo et al. (2014). The vegetation cover (ET) in most basins is denser (higher)  
405 than that in the westerlies-dominant basins. Moreover, the seasonal snow mainly  
406 covers from mid-autumn to spring and correspondingly the SWE is relatively higher  
407 in these months in all basins except for Yellow River above Xining station, Salwee  
408 River above Jiayuqiao station and Brahmaputra River above Nuxia and Yangcun  
409 stations.

410 < Figure 7, here please, thanks >

### 411 **3.3 Trends of basin-wide water budget components for the TP basins**

412 The Q, P and  $ET_{wb}$  overall ascended under regional warming during the past 30  
413 years in the westerlies-dominated basins (Fig.8) except for P in the Yerqiang River  
414 basin (Kulukelangan station), but only Q in Keliya River basin (Numaitilangan station)  
415 showed statistically significantly increase at the 0.05 level. The aridity index (PET/P),  
416 which is an indicator for the degree of dryness, slightly declined (not significant) in  
417 all basins in northwestern TP. Although both P and PET increased in the Keliya River  
418 basin since the 1980s (Shi et al., 2003; Yao et al., 2014), the PET/P declined due to the  
419 higher rates of the increase of P than that of PET. The climate moistening (Shi et al.,  
420 2003) in the headwaters of these inland rivers would be beneficial to the water  
421 resources and oasis agro-ecosystems in the middle and lower basins. The increase in  
422 streamflow was also found in most tributaries of the Tarim River (Sun et al., 2006; Fu

423 et al., 2010; Mamat et al., 2010). Moreover, the westerlies, revealed by the Asian  
424 Zonal Circulation Index (60°-150° E), slightly enhanced (linear trend: 0.21, P-value:  
425 0.26) over the period 1982-2011 (Fig.9). With the strengthening westerlies, more  
426 water vapor may be transported and fell as rain or snow in northwestern TP (e.g., the  
427 eastern Pamir region). Both SWE products (VIC\_IGSNRR simulated and  
428 GlobaSnow-2 product) showed marginally increase across these basins with rising  
429 seasonal snow covers and glaciers (Yao et al., 2012). More precipitation was  
430 transformed into snow/glacier and the runoff coefficient (Q/P) exhibited decrease with  
431 precipitation obviously increased (Fig.8). In addition, the transpiration in these basins  
432 might overall decrease with vegetation degradation (Yin et al., 2016) as revealed by  
433 the NDVI and LAI (both decrease significantly in all westerlies-dominated basins  
434 except NDVI in Yerqiang and Yulongkashi rivers) but the atmospheric evaporative  
435 demand indicated by CRU PET increased (significantly increase in the Yulongkashi  
436 and Keliya rivers) during the period 1982-2011.

437 < Figure 8, here please, thanks>

438 < Figure 9, here please, thanks>

439 In the East Asian monsoon dominated basins, there are two types of change for  
440 basin-wide water budget components. For example, P and Q showed marginally  
441 decrease in the upper Yellow River (Tangnihai, Huangheyuan and Jimai stations) and  
442 Yalong River (Yajiang station) but slightly increased in other basins (Zelingou,  
443 Gandatan, Xining, Tongren and Zhimenda stations) over the period of 1982-2011  
444 (Fig.10). Only P in Zhimenda station exhibited statistically significant increase at the  
445 0.05 level. The declined Q and P in the upper Yellow and Yalong Rivers (located at the  
446 eastern Tibetan Plateau) were consistent with that found by Cuo et al. (2013, 2014)  
447 and Yang et al. (2014), and were in line with the weakening East Asian Summer

448 Monsoon (linear slope: -0.01, P-value: 0.56) (Fig.9). The vegetation turned green  
449 markedly while  $ET_{wb}$  and PET increased (distinctly trends were found for  $ET_{wb}$  in  
450 basins controlled by Zelingou, Tangnaihai and Zhimenda and for PET in all rivers  
451 except for basins controlled by Xining, Tongren and Zhimenda stations) in all East  
452 Asian-monsoon dominated basins except for  $ET_{wb}$  in basins above Tongren and  
453 Yajiang stations with the ascending air temperature during the period 1982-2011. The  
454 aridity index (PET/P) slightly decreased in all basins (significantly decrease was  
455 found in the upper Yangtze River basin above Zhimenda station) except for the upper  
456 Yellow River basin above Jimai station and the upper Yalong River basin above  
457 Yajiang station. Moreover, the SWE showed slight but insignificant decrease in most  
458 East Asian monsoon dominated basins (SWE\_VIC exhibited markedly decline in  
459 basins above Tangnaihai, Huangheyan and Zhimenda stations while SWE\_Globsnow  
460 showed significantly decrease in basins above Xining station) except for the Bayin  
461 River above Zelingou station and the upper Yellow River above Tongren station.

462 < Figure 10, here please, thanks >

463 The P,  $ET_{wb}$  and Q increased slightly in the Indian monsoon-dominated basins  
464 (except for  $ET_{wb}$  in the basin above Yangcun station) (Fig.11), which are in line with  
465 the strengthening (linear trend: 0.01, P-value: 0.12) of the Indian summer monsoon  
466 (revealed by the Indian Ocean Dipole Mode Index) during the specific period  
467 1982-2011 (Fig.9). However, only P in basins above Nuxia and Yangcun stations, Q in  
468 Nuxia station as well as  $ET_{wb}$  in basins above Jiayuqiao, Pangduo, Tangjia and  
469 Yangcun showed statistically significant trends at the 0.05 level. The slightly  
470 increasing trend of annual streamflow at Jiayuqiao station was consistent with that  
471 examined by Yao et al. (2012) during the period 1980-2000. The vegetation status,  
472 revealed by NDVI and LAI, turned better slightly (markedly trends were found in

473 NDVI in basin above Gongbujiangda stations and LAI in all Indian  
474 monsoon-dominated basins except for one above Pangduo station) associated with the  
475 ascending air temperature. The aridity index (PET/P) exhibited slight but insignificant  
476 decrease in all basins (markedly declined in basins above Nuxia and Yangcun stations)  
477 except for the Brahmaputra River above Tangjia station, which indicated that most  
478 basins in the Indian monsoon-dominated regions turned wetter over the period of  
479 1982-2011. The increased PET/P in Brahmaputra River basin may be consistent with  
480 the drying moisture flux in the southeastern TP, as illustrated by Gao et al. (2014).  
481 The runoff coefficient (Q/P) slightly increased in basins above Gongbujiangda and  
482 Nuxia stations while distinctly decreased in basins above Jiayuqiao, Tangji and  
483 Yangcun stations. Moreover, the basin-wide SWE\_Globsnow exhibited minor  
484 decrease in the upper Salween River and Brahmaputra River above Tangjia and  
485 Gongbujiangda stations while significantly increased in Brahmaputra River above  
486 Nuxia and Yangcun stations.

487 < Figure 11, here please, thanks >

### 488 **3.4 Uncertainties**

489 The results may unavoidably associate with some uncertainties inherited from the  
490 multi-source datasets used. The primary sources of uncertainty may arise from the  
491 precipitation inputs. We compared the seasonal cycles and annual trends in different  
492 precipitation products, i.e. CMA\_P, IGSNRR\_P and TRMM\_P (and their  
493 calculated  $ET_{wb}$  from the water balance) during the period 2000-2011 (Fig. 12 and  
494 Fig. 13). We found there are some uncertainties among different precipitation  
495 products and thus among their estimated  $ET_{wb}$ , especially in the westerlies-dominated  
496 basins. However, for each basin, the seasonal cycles of precipitation (and their  
497 calculated  $ET_{wb}$ ) calculated from different products are overall similar (especially for

498 the observation-based products, CMA\_P and IGSNRR\_P). The signs of trend for  
499 annual CMA\_P and IGSNRR\_P (and their calculated  $ET_{wb}$ ) are consistent in most  
500 river basins (i.e., 14 out 18 basins for two precipitation products and 17 out 18 basins  
501 for their calculated  $ET_{wb}$ ) during the period 1982-2011. The consistency of trends  
502 between two precipitation products, to some extent, revealed that the trends in  
503 CMA\_P were not obviously influenced by the changing density of rain gauges in TP  
504 basins. Although some uncertainties exist due to limited and unevenly distributed  
505 meteorological stations used in the plateau and the influences of complex terrain,  
506 CMA\_P is still the best observation-based precipitation product nowadays in China  
507 which could be applied to hydrological studies in the TP.

508 < Figure 12, here please, thanks >

509 < Figure 13, here please, thanks >

510 Although the seasonal cycles of  $ET_{wb}$  could be captured by GLEAM\_E and VIC\_E,  
511 they still have considerable uncertainties at some stations (e.g., Numaitilangan,  
512 Gongbujiangda and Nuxia) (Fig.5). Compared to the annual trend of  $ET_{wb}$  (Table 4),  
513 most ET products (including the well-performed GLEAM\_E and VIC\_E) could not  
514 detect the decreasing trends in 7 out of 18 basins (Kulukelangan, Tongguziluoke,  
515 Xining, Tongren, Jimai, Nuxia and Gongbujiangda) due to their different forcing data,  
516 algorithm used as well as varied spatial-temporal resolutions (Xue et al., 2013; Li et  
517 al., 2014; Liu et al., 2016a). In particular, it is well known that land surface models  
518 have some difficulties (e.g., parameter tuning in boundary layer schemes) when  
519 applying to the TP, even though they sometimes have good performances in different  
520 regions/basins (Xia et al., 2012; Bai et al., 2016). For example, Xue et al. (2013)  
521 indicated that GNoah\_E underestimated the  $ET_{wb}$  in the upper Yellow River and  
522 Yangtze River basins on the Tibetan Plateau mainly due to its negative-biased

523 precipitation forcing. We thus only used  $ET_{wb}$  in the trend detection of water budget  
524 components in Fig.8, Fig.10 and Fig.11 in this study. The two SWE products also  
525 showed large uncertainty with respect to both their seasonal cycles and trends. The  
526 VIC\_IGSNRR simulated and GlobaSnow-2 SWEs have not been validated in the TP  
527 due to the lack of snow water equivalent observations, but in some basins (e.g.,  
528 Zelingou and Numaitilangan) they showed similar seasonal cycles and annual trends.

529 <Table 4, here please, thanks>

530 The interpolation of missing values of runoff with VIC\_IGSNRR simulated runoff  
531 and the gridded precipitation data (which interpolated from limited gauged  
532 precipitation over the plateau) also introduced uncertainties. There are also  
533 considerable uncertainties arising from empirical extending the ET series back prior  
534 to the GRACE era. However, the trends in  $ET_{wb}$  have not significantly affected by  
535 erroneous trends in the precipitation inputs to the bias-correction based water balance  
536 calculation. For example, the trends in CMA\_P and IGSNRR\_P are opposite in few  
537 basins (No. 01, 07, 08, 13 in Fig. 13), but the trends in their calculated  $ET_{wb}$  are both  
538 consistent for each basin. It is, to some extent, certified the effectiveness of the bias  
539 correction-based ET-estimate approach. With these caveats, we can interpret the  
540 general hydrological regimes and their responses to the changing climate in the TP  
541 basins from solely the perspective of multi-source datasets, which are comparable to  
542 the existing studies based on the in situ observations and complex hydrological  
543 modeling.

544

#### 545 **4 Summary**

546 In this study, we investigated the seasonal cycles and trends of water budget  
547 components in 18 TP basins during the period 1982-2011, which is not well

548 understood so far due to the lack of adequate observations in the harsh environment,  
549 through integrating the multi-source global/regional datasets such as gauge data,  
550 satellite remote sensing and land surface model simulations. By using a two-step bias  
551 correction procedure, we calculated the annual basin-wide  $ET_{wb}$  through the water  
552 balance approach considering the impacts of water storage change. We found that the  
553 GLEAM\_E and VIC\_E perform better relative to other products against the  
554 calculated  $ET_{wb}$ .

555

556 From the Budyko framework perspective, the general water and energy budgets are  
557 different in the westerlies-dominated (with higher aridity index, runoff coefficient and  
558 glacier cover), the Indian monsoon-dominated and the East Asian  
559 monsoon-dominated (with higher air temperature, vegetation cover and  
560 evapotranspiration) basins. In the 18 TP basins, precipitation is the major contributor  
561 to the river runoff, which concentrates mainly during June-October (June-August for  
562 the westerlies-dominated basins, June-September or June to October for the Indian  
563 monsoon-dominated and the East Asian monsoon-dominated basins). The basin-wide  
564 SWE is relatively high from mid-autumn to spring for all 18 TP basins except for  
565 Keliya River and Brahmaputra River above the Nuxia and Yangcun stations. The  
566 vegetation cover is relatively less whereas snow/glacier cover is more in the  
567 westerlies-dominant basins compared to other basins.

568

569 During the period 1982-2011, the P, Q and  $ET_{wb}$  showed slight but insignificant  
570 increase across most of the basins in Tibetan Plateau with the exception of some  
571 tributaries located at the upper Yellow River and Yalong River due to the weakening  
572 East Asian monsoon. The aridity index (PET/P) exhibited an indistinctively

573 decreasing trend in most TP basins which corresponds to the warming and moistening  
574 climate in the TP and western China. Moreover, the runoff coefficient (Q/P) declined  
575 marginally in most basins which may be, to some extent, due to ET increase induced  
576 by vegetation greening and the influences of snow and glacier changes. Although  
577 there are considerable uncertainties inherited from multi-source data used, the general  
578 hydrological regimes in the TP basins could be revealed, which are consistent to the  
579 existing results obtained from in situ observations and complex land surface modeling.  
580 It indicates the usefulness of integrating the multiple datasets (e.g., in situ  
581 observations, remote sensing-based products, reanalysis outputs, land surface model  
582 simulations and climate model outputs) for hydrological applications. The  
583 generalization here could be helpful for understanding the hydrological cycle and  
584 supporting sustainable water resources management and eco-environment protection  
585 in the Tibetan Plateau.

586

587 ***Author contributions.*** Wenbin Liu and Fubao Sun developed the idea to see the  
588 general water budgets in the TP basins from the perspective of multisource datasets.  
589 Wenbin Liu collected and processed the multiple datasets with the help of Yanzhong  
590 Li, Guoqing Zhang, Wee Ho Lim, Hong Wang as well as Peng Bai, and prepared the  
591 manuscript. The results were extensively commented and discussed by Fubao Sun,  
592 Jiahong Liu and Yan-Fang Sang.

593

594 ***Acknowledgements.*** This study was supported by the National Key Research and  
595 Development Program of China (2016YFC0401401 and 2016YFA0602402), National  
596 Natural Science Foundation of China (41401037, 41601035, 91647110, 41701019  
597 and 41330529), the Open Research Fund of State Key Laboratory of Desert and Oasis  
598 Ecology in Xinjiang Institute of Ecology and Geography, Chinese Academy of



599 Sciences (CAS), the Key Research Program of the CAS (ZDRW-ZS-2017-3-1), the  
600 CAS Pioneer Hundred Talents Program (Fubao Sun), the CAS President's  
601 International Fellowship Initiative (2017PC0068) and the program for the "Bingwei"  
602 Excellent Talents from the Institute of Geographic Sciences and Natural Resources  
603 Research, CAS. We are grateful to the NASA MEaSUREs Program (Sean Swenson)  
604 for providing the GRACE land data processing algorithm. The basin-wide water  
605 budget series in the TP Rivers used in this study are available from the authors upon  
606 request ([liuwb@igsnr.ac.cn](mailto:liuwb@igsnr.ac.cn)). We thank Axel Kleidon, the editors and reviewers for  
607 their invaluable comments and constructive suggestions.

608

## 609 **References**

- 610 Akhtar, M., Ahmad, N., and Booij, M.J.: Use of regional climate model simulations as input for  
611 hydrological models for the Hindukush-Karakorum-Himalaya region, *Hydrol. Earth Syst. Sci.*  
612 13, 1075-1089, 2009.
- 613 Bai, P., Liu, X.M., Yang, T.T., Liang, K., and Liu, C.M.: Evaluation of streamflow simulation  
614 results of land surface models in GLDAS on the Tibetan Plateau, *J. Geophys. Res. Atmos.*, 121,  
615 12180-12197, 2016.
- 616 Berrisford, P, Lee, D., Poli, P., Brugge, R., Fielding, K., Fuentes, M., Kallberg, P., Kobayashi, S.,  
617 Uppala, S., and Simmons, A.: The ERA-interim archive. ERA Reports Series No. 1 Version 2.0,  
618 Available from: <[https://www.researchgate.net/publication/41571692\\_The\\_ERA-interim](https://www.researchgate.net/publication/41571692_The_ERA-interim_archive)  
619 archive>, 2011.
- 620 Bookhagen, B. and Burbank, D.W.: Toward a complete Himalayan hydrological budget:  
621 spatiotemporal distribution of snowmelt and rainfall and their impact on river discharge, *J.*  
622 *Geophys. Res.*, 115, F03019, 2010.
- 623 Bouraoui, F., Vachaud, G., Li, L.Z.X., LeTreut, H., and Chen, T.: Evaluation of the impact of  
624 climate changes on water storage and groundwater recharge at the watershed scale, *Clim. Dyn.*,  
625 15(2), 153-161, 1999.
- 626 Budyko, M.I.: *Climate and life*. Academic Press, 1974.

627 Chen, D., Xu, B., Yao, T., Guo, Z., Cui, P., Chen, F., Zhang, R., Zhang, X., Zhang, Y., Fan, J., Hou,  
628 Z., and Zhang, T.: Assessment of past, present and future environmental changes on the Tibetan  
629 Plateau, *Chinese SCI. Bull.*, 60(32), 3025-3035, 2015 (in Chinese).

630 Cuo, L., Zhang, Y.X., Bohn, T.J., Zhao, L., Li, J.L., Liu, Q.M., and Zhou, B.R.: Frozen soil  
631 degradation and its effects on surface hydrology in the northern Tibetan Plateau, *J. Geophys.*  
632 *Res. Atmos.*, 120(6), 8276-8298, 2015.

633 Cuo, L., Zhang, Y.X., Gao, Y., Hao, Z., and Cairang, L.: The impacts of climate change and land  
634 cover/use transition on the hydrology in the upper Yellow River Basin, China, *J. Hydrol.*, 502,  
635 37-52, 2013.

636 Cuo, L., Zhang, Y.X., Zhu, F.X., and Liang, L.Q.: Characteristics and changes of streamflow on  
637 the Tibetan Plateau: A review, *J. Hydrol. Reg. stud.*, 2, 49-68, 2014.

638 Dong, X., Yao, Z., and Chen, C.: Runoff variation and responses to precipitation in the source  
639 regions of the Yellow River, *Resour. Sci.*, 29(3), 67-73, 2007 (in Chinese).

640 Dong, W., Lin, Y., Wright, J.S., Ming, Y., Xie, Y., Wang, B., Luo, Y., Huang, W., Huang, J., Wang,  
641 L., Tian, L., Peng, Y., and Xu, F.: Summer rainfall over the southwestern Tibetan Plateau  
642 controlled by deep convection over the Indian Subcontinent, *Nat. Commun.*, 7, 10925, 2016.

643 Duan, A.M. and Wu, G.X.: Change of cloud amount and the climate warming on the Tibetan  
644 Plateau, *Geophys. Res. Lett.*, 33, L22704, 2006.

645 Fu, L., Chen, Y., Li, W., Xu, C., and He, B.: Influence of climate change on runoff and water  
646 resources in the headwaters of the Tarim River, *Arid Land Geogr.*, 31(2), 237-242, 2008 (in  
647 Chinese).

648 Fu, L., Chen, Y., Li, W., He, B., and Xu, C.: Relation between climate change and runoff volume  
649 in the headwaters of the Tarim River during the last 50 years., *J. Desert Res.*, 30(1), 204-209,  
650 2010 (in Chinese).

651 Gao, Y.H., Cuo, L., and Zhang, Y.X.: Changes in moisture flux over the Tibetan Plateau during  
652 1979-2011 and possible mechanisms, *J. Climate*, 27, 1876-1893, 2014.

653 Guo, W.Q., Liu, S.Y., Yao, X.J., Xu, J.L., Shangguan, D.H., Wu, L.Z., Zhao, J.D., Liu, Q., Jiang,  
654 Z.L., Wei, J.F., Bao, E.J., Yu, P.C., Ding, L.F., Li, G., Ge, C.M., and Wang, Y.: The Second  
655 Glacier Inventory Dataset of China, Cold and Arid Regions Science Data Center at Lanzhou,  
656 doi: 10.3972/glacier.001.2013.db, 2014.

657 Hamed, K.H. and Rao, A.R.: A modified Mann-Kendall trend test for autocorrelation data,  
658 J.Hydrol., 204(1-4), 182-196, 1998.

659 Huffman, G.J., , E.F., Bolvin, D.T., Nelkin, E.J., and Adler, R.F.: last updated 2013: TRMM  
660 Version 7 3B42 and 3B43 Data Sets, NASA/GSFC, Greenbelt, MD. Data set accessed at  
661 [http://mirador.gsfc.nasa.gov/cgi-bin/mirador/](http://mirador.gsfc.nasa.gov/cgi-bin/mirador/presentNavigation.pl?tree=project&project=TRMM&dataGroup=Gridded&CGIS)  
662 [presentNavigation.pl?tree=project&project=TRMM&dataGroup=Gridded&CGIS](http://mirador.gsfc.nasa.gov/cgi-bin/mirador/presentNavigation.pl?tree=project&project=TRMM&dataGroup=Gridded&CGIS)  
663 [ESSID=5d12e2ffa38ca2aac6262202a79d882a](http://mirador.gsfc.nasa.gov/cgi-bin/mirador/presentNavigation.pl?tree=project&project=TRMM&dataGroup=Gridded&CGIS), 2012.

664 Harris, I., Jones, P.D., Osborn, T.J., and Lister, D.H.: Updated high-resolution grids of monthly  
665 climatic observations – the CRU TS3.10 Dataset, *Int. J. Climatol.*, 34 (3), 623-642, 2014.

666 Immerzeel, W.W., van Beek, L.P.H., and Bierkens, M.F.P.: Climate change will affect the Asian  
667 water towers, *Science*, 328, 1382-1385, 2010.

668 Jung, M., Reichstein, M., Ciais, P., Seneviratne, S.I., Sheffield, J., Goulden, M.L., Bonan, G.,  
669 Cescatti, A., Chen, J., de Jeu, R., Dolman, A.J., Eugster, W., Gerten, D., Gianelle, D., Gobron, N.,  
670 Heinke, J., Kimball, J., Law, B.E., Montagnani, L., Mu, Q., Mueller, B., Oleson, K., Papale, D.,  
671 Richardson, A.D., Rouspard, O., Running, S., Tomelleri, E., Viovy, N., Weber, U., Williams, C.,  
672 Wood, E., Zaehle, S., and Zhang, K.: Recent decline in the global land evapotranspiration trend  
673 due to limited moisture supply, *Nature*, 467, 951-954, 2010.

674 Kobayashi, S., Ota, Y., Harada, Y., Ebata, A., Moriya, M., Onoda, H., Onogi, K., kamahori, H.,  
675 kobayashi, C., Endo, H., miyaoka, K., and Takahashi, K.: The JRA-55 Reanalysis: General  
676 specifications and basic characteristics, *J.Meteor. Soc. Japan*, 93(1), 5-58, doi:  
677 10.2151/jmsj.2015-001, 2015.

678 Landerer, F.W. and Swenson, S.C.: Accuracy of scaled GRACE terrestrial water storage estimates,  
679 *Water Resour.Res.*, 48, W04531, 2012.

680 Li, F.P., Zhang, Y.Q., Xu, Z.X., Liu, C.M., Zhou, Y.C., and Liu, W.F.: Runoff predictions in  
681 ungauged catchments in southeast Tibetan Plateau, *J. Hydrol.*, 511, 28-38, 2014.

682 Li, F.P., Zhang, Y.Q., Xu, Z.X., Teng, J., Liu, C.M., Liu, W.F., and Mpelasoka, F.: The impact of  
683 climate change on runoff in the southeastern Tibetan Plateau, *J. Hydrol.*, 505, 188-201, 2013.

684 Li, J.P. and Zeng, Q.C.: A unified monsoon index, *Geophys. Res. Lett.*, 29(8), 1274, 2002.

685 Li, X.P., Wang, L., Chen, D.L., Yang, K., and Wang, A.H.: Seasonal evapotranspiration changes  
686 (1983-2006) of four large basins on the Tibetan Plateau, *J. Geophys. Res.*, 119 (23),  
687 13079-13095, 2014.

688 Liang, S.L. and Xiao, Z.Q.: Global Land Surface Products: Leaf Area Index Product Data  
689 Collection(1985-2010), Beijing Normal University, doi:10.6050/glass863.3004.db, 2012.

690 Liu, T.: Hydrological characteristics of Yalungzangbo River, *Acta Geogr. Sin.*, 54 (Suppl.),  
691 157-164, 1999 (in Chinese).

692 Liu, W.B. and Sun, F.B.: Assessing estimates of evaporative demand in climate models using  
693 observed pan evaporation over China, *J. Geophys. Res. Atmos.*, 121, 8329-8349, 2016.

694 Liu, W.B., Wang, L., Zhou, J., Li, Y.Z., Sun, F.B., Fu, G.B., Li, X.P., and Sang, Y-F.: A worldwide  
695 evaluation of basin-scale evapotranspiration estimates against the water balance method, *J.*  
696 *Hydrol.*, 538, 82-95, 2016a.

697 Liu, W.B., Wang, L., Chen, D.L., Tu, K., Ruan, C.Q., and Hu, Z.Y.: Large-scale circulation  
698 classification and its links to observed precipitation in the eastern and central Tibetan Plateau,  
699 *Clim. Dyn.*, 46, 3481-3497, 2016b.

700 Liu, X.M., Yang, T., Hsu, K., Liu, C., and Sorooshian, S.: Evaluating the streamflow simulation  
701 capability of PERSIANN-CDR daily rainfall products in two river basins on the Tibetan Plateau,  
702 *Hydrol. Earth Syst. Sci.*, 21, 169-181, 2017.

703 Long, D., Shen, Y.J., Sun, A., Hong, Y., Longuevergne, L., Yang, Y.T., Li, B., and Chen, L.:  
704 Drought and flood monitoring for a large karst plateau in Southwest China using extended  
705 GRACE data, *Remote Sens. Environ.*, 155, 145-160, 2014.

706 Lucchesi, R.: File specification for MERRA products, GMAO Office Note No.1 (version 2.3), 82  
707 pp, available from [http://gmao.gsfc.nasa.gov/pubs/office\\_notes](http://gmao.gsfc.nasa.gov/pubs/office_notes), 2012.

708 Ma, N., Szilagyi, J., Niu, G.Y., Zhang, Y.S., Zhang, T., Wang, B.B., and Wu, Y.H.: Evaporation  
709 variability of Nam Co Lake in the Tibetan Plateau and its role in recent rapid lake expansion, *J.*  
710 *Hydrol.*, 537, 27-35, 2016.

711 Ma, N., Zhang, Y.S., Guo, Y.H., Gao, H.F., Zhang, H.B., and Wang, Y.F.: Environmental and  
712 biophysical controls on the evapotranspiration over the highest alpine steppe, *J. Hydrol.*, 529,  
28 / 57

713 980-992, 2015.

714 Mamat, A., Halik, W., and Yang, X.: The climatic changes of Qarqan river basin and its impact on  
715 the runoff, *Xinjiang Agric. Sci.*, 47 (5), 996-1001, 2010 (in Chinese).

716 McVicar, T.R., Roderick, M., Donohue, R.J., Li, L.T., Van Niel, T.G., Thomas, A., Grieser, J.,  
717 Jhajharia, D., Himri, Y., Mahowald, N.M., Mescherskaya, A.V., Kruger, A.C., Rehman, S., and  
718 Dinpashoh, Y.: Global review and synthesis of trends in observed terrestrial near-surface wind  
719 speeds: implications for evaporation, *J. Hydrol.*, 416-417, 182-205, 2012.

720 Miralles, D.G., De Jeu, R.A.M., Gash, J.H., Holmes, T.R.H., and Dolman, A.J.: Magnitude and  
721 variability of land evaporation and its components at the global scale, *Hydrol. Earth Syst. Sci.*, 15,  
722 967-981, 2011.

723 Miralles, D.G., Gash, J.H., Holmes, T.R.H., de Jeu, R.A.M, and Dolman, A.J.: Global canopy  
724 interception from satellite observations, *J. Geophys. Res.*, 115, D16122, 2010.

725 Oliveira, P.T.S., Mearing, M.A., Moran, M.S., Goodrich, D.C., Wendland, E., and Gupta, H.V.:  
726 Trends in water balance components across the Brazilian Cerrado, *Water Resour. Res.*, 50,  
727 7100-7114, 2014.

728 Rodell, M., Houser, P.R., Jambor, U., Gottschalck, J., Mitchell, K., Meng, C.-J., Arsenault, K.,  
729 Cosgrove, B., Radakovich, J., Bosilovich, M., Entin, J.K., Walker, P., Lohmann, D., and Toll, D.:  
730 The global land data assimilation system, *B. Am. Meteorol. Soc.*, 85, 381-394, 2004.

731 Rui, H.: README Document for Global Land Data Assimilation System Version 2 (GLDAS-2)  
732 Products, GES DISC, 2011.

733 Saji, N.H., Goswami, B.N., Vinayachandran, P.N., and Yamagata, T.: A dipole mode in the tropical  
734 Indian Ocean, *Nature*, 401, 360-363, 1999.

735 Shen, M.G., Piao, S.L., Jeong, S., Zhou, L.M., Zeng, Z.Z., Ciais, P., Chen, D.L., Huang, M.T., Jin,  
736 C.S., Li, L.Z.X., Li, Y., Myneni, R.B., Yang, K., Zhang, G.X., Zhang, Y.J., and Yao, T.D.:  
737 Evaporative cooling over the Tibetan Plateau induced by vegetation growth, *Proc. Natl. Acad.*  
738 *Sci. U. S.A.*, 112(30), 9299-9304, 2015.

739 Shi, Y.F., Shen, Y.P., Li, D.L., Zhang, G.W., Ding, Y.J., Hu, R.J., and Kang, E.S.: Discussion on  
740 the present climate change from Warm2dry to Warm2wet in northwest China, *Quat. Sci.*, 23(2),  
741 152-164, 2003 (in Chinese).

742 Shepard, D.S.: Computer mapping: the SYMAP interpolation algorithm. *Spatial Statistics and*  
**29 / 57**

743 Models, G.L. Gaile and C.J. Willmott, Eds., D. Reidel, 133-145, 1984.

744 Sun, B., Mao, W., Feng, Y., Chang, T., Zhang, L., and Zhao, L.: Study on the change of air  
745 temperature, precipitation and runoff volume in the Yarkant River basin, *Arid Zone Res.*, 23(2),  
746 203-209, 2006 (in Chinese).

747 Takala, M., Luojus, K., Pulliainen, J., Derksen, C., Lemmetyinen, J., Kärnä J.-P., Koskinen, J., and  
748 Bojkov, B.: Estimating northern hemisphere snow water equivalent for climate research through  
749 assimilation of spaceborne radiometer data and ground-based measurements, *Remote  
750 Sens. Environ.*, 115 (12), 3517-3529, 2011.

751 Tapley, B.D., Bettadpur, S., Watkins, M., and Reigber, C.: The gravity recovery and climate  
752 experiment: mission overview and early results, *Geophys. Res. Lett.*, 31, L09607, 2004.

753 Tian, L., Yao, T., MacClune, K., White, J.W.C., Schilla, A., Vaughn, B., Vachon, R., and  
754 Ichiyonagi, K.: Stable isotopic variations in west China: a consideration of moisture sources, *J.  
755 Geophys. Res. Atmos.*, 112, D10112, 2007.

756 Tucker, C.J., Pinzon, J.E., Brown, M.E., Slayback, D., Pak, E.W., Mahoney, R., Vermote, E., and  
757 El Saleous, N.: An extended AVHRR 8 km NDVI data set compatible with MODIS and SPOT  
758 vegetation NDVI data, *Int. J. Remote Sens.*, 26(20), 4485-4498, 2005.

759 von Storch, H.: Misuses of statistical analysis in climate research, In *Analysis of Climate  
760 Variability: Applications of Statistical Techniques*, Springer-Verlag: Berlin, 11-26, 1995.

761 Wang, A. and Zeng, X.: Evaluation of multireanalysis products within site observations over the  
762 Tibetan Plateau, *J. Geophys. Res.*, 117, D05102, 2012.

763 Wang, L., Sun, L.T., Shrestha, M., Li, X.P., Liu, W.B., Zhou, J., Yang, K., Lu, H., and Chen, D.L.:  
764 Improving snow process modeling with satellite-based estimation of  
765 near-surface-air-temperature lapse rate, *J. Geophys. Res. Atmos.*, 121, 12005-12030, 2016.

766 Xia, Y., Mitchell, K., Ek, M., Cosgrove, B., Sheffield, J., Luo, L., Alonge, C., Wei, H., Meng, J.,  
767 Livneh, B., and Duang, Q.: Continental-scale water and energy flux analysis and validation for  
768 North American Land Data Assimilation System project phase 2 (NLDAS-2): 2. Validation of  
769 model-simulated streamflow, *J. Geophys. Res. Atmos.*, 117(D3), D03110, 2012.

770 Xu, L.: The land surface water and energy budgets over the Tibetan Plateau, Available from

771 Nature Precedings < <http://hdl.handle.net/10101/npre.2011.5587.1>>, 2011.

772 Xue, B.L., Wang, L., Yang, K., Tian, L., Qin, J., Chen, Y., Zhao, L., Ma, Y., Koike, T., Hu, Z., and  
773 Li, X.P.: Modeling the land surface water and energy cycle of a mesoscale watershed in the  
774 central Tibetan Plateau with a distributed hydrological model, *J. Geophys. Res. Atmos.*, 118,  
775 8857-8868, 2013.

776 Yao, Z., Duan, R., and Liu, Z.: Changes in precipitation and air temperature and its impacts on  
777 runoff in the Nujiang River basins. *Resour. Sci.* 34(2), 202-210, 2012 (in Chinese)

778 Yang, K., Qin, J., Zhao, L., Chen, Y.Y., Tang, W.J., Han, M.L., Lazhu, Chen, Z.Q., Lv, N., Ding,  
779 B.H., Wu, H., and Lin, C.G.: A multi-scale soil moisture and freeze-thaw monitoring network  
780 on the third pole, *Bull. Am. Meteorol. Soc.*, 94,1907-1916, 2013.

781 Yang, K., Wu, H., Qin, J., Lin, C.G., Tang, W.J., and Chen, Y.Y.: Recent climate changes over the  
782 Tibetan Plateau and their impacts on energy and water cycle: a review, *Glob. Planet Change*,  
783 112, 79-91, 2014.

784 Yao, T.D., Thompson, L., Yang, W., Yu, W.S., Gao, Y., Guo, X.J., Yang, X.X., Duan, K.Q., Zhao,  
785 H.B., Xu, B.Q., Pu, J.C., Lu, A.X., Xiang, Y., Kattel, D.B., and Joswiak, D.: Different glacier  
786 status with atmospheric circulations in Tibetan Plateau and surroundings, *Nat. Clim. Change*, 2,  
787 1-5, 2012.

788 Yao, Y.J., Zhao, S.H., Zhang, Y.H., Jia, K., and Liu, M.: Spatial and decadal variations in potential  
789 evapotranspiration of China based on reanalysis datasets during 1982-2010, *Atmosphere*, 5,  
790 737-754, 2014.

791 Yin, G., Hu, Z.Y., Chen, X., and Tiyip, T.: Vegetation dynamics and its response to climate change  
792 in Central Asia, *J. Arid Land*, 8, 375, 2016.

793 Yu, J., Zhang, G., Yao, T., Xie, H., Zhang, H., Ke, C., and Yao, R.: Developing daily cloud-free  
794 snow composite products from MODIS Terra-Aqua and IMS for the Tibetan Plateau, *IEEE*  
795 *Trans. Geosci. Remote Sens.*, 54(4), 2171-2180, 2015.

796 Yue, S., Pilon, P., Phinney, B., Cavadias, G.: The influence of autocorrelation on the ability to  
797 detect trend in hydrological series, *Hydrol. Process.*, 16(9), 1807-1829, 2002.

798 Zhang, D., Liu, X., Zhang, Q., Liang, K., and Liu, C.: Investigation of factors affecting  
799 inter-annual variability of evapotranspiration and streamflow under different climate conditions.  
800 *J. Hydrol.*, 543, 759-769, 2016.

801 Zhang, G., Xie, H., Yao, T., Liang, T., and Kang, S.: Snow cover dynamics of four lake basins  
802 over Tibetan Plateau using time series MODIS data (2001-2100), *Water Resour. Res.*, 48(10),  
803 W10529, 2012.

804 Zhang, K., Kimball, J.S., Nemani, R.R., and Running, S.W.: A continuous satellite-derived global  
805 record of land surface evapotranspiration from 1983 to 2006, *Water Resour. Res.*, 46(9),  
806 W09522, 2010.

807 Zhang, L., Su, F., Yang, D., Hao, Z., and Tong, K.: Discharge regime and simulation for the  
808 upstream of major rivers over Tibetan Plateau, *J. Geophys. Res. Atmos.*, 118(15), 8500-8518,  
809 2013.

810 Zhang, Q., Li, J., Singh, V., and Xu, C.: Copula-based spatial-temporal patterns of precipitation  
811 extremes in China, *Int. J. Climatol.*, 33, 1140-1152, 2013.

812 Zhang, X., Tang, Q., Pan, M., and Tang, Y.: A long-term land surface hydrologic fluxes and states  
813 dataset for China, *J. Hydrometeorol.*, 15, 2067-2084, 2014.

814 Zhang, Y., Peña-Arancibia, J.L., McVicar, T.R., Chiew, F.H.S., Vaze, J., Liu, C.M., Lu, X.J.,  
815 Zheng, H.X., Wang, Y.P., Liu, Y.Y., Miralles, D.G., and Pan, M.: Multi-decadal trends in global  
816 terrestrial evapotranspiration and its components, *Scientific Reports*, 6, 19124, 2016.

817 Zhang, Y., Liu, C., Tang, Y., and Yang, Y.: Trend in pan evaporation and reference and actual  
818 evapotranspiration across the Tibetan Plateau, *J. Geophys. Res.*, 112, D12110, 2007.

819 Zhou, C., Jia, S., Yan, H., and Yang, G.: Changing trend of water resources in Qinghai Province  
820 from 1956 to 2000, *J. Glaciol. Geocryol.*, 27(3), 432-437, 2005 (in Chinese).

821 Zhou, J., Wang, L., Zhang, Y.S., Guo, Y.H., Li, X.P., and Liu, W.B.: Exploring the water storage  
822 changes in the largest lake (Selin Co) over the Tibetan Plateau during 2003-2012 from a  
823 basin-wide hydrological modeling., *Water Resour. Res.*, 51, 8060-8086, 2015.

824 Zhou, S.Q., Kang, S., Chen, F., and Joswiak, D.R.: Water balance observations reveal significant  
825 subsurface water seepage from Lake Nam Co., south-central Tibetan Plateau., *J. Hydrol.*, 491,  
826 89-99, 2013.

827 Zhu, Y., Chen, J., Chen, G.: Runoff variation and its impacting factors in the headwaters of the  
828 Yangtze River in recent 32 years, *J. Yangtze River Sci. Res. Inst.*, 28(6), 1-4, 2011 (in Chinese ).



829 **Table 1:** Overview of multi-source datasets applied in this study

Data category	Data source	Spatial resolution	Temporal resolution	Available period used	Reference
Runoff (Q)	Observed, National Hydrology Almanac of China	—	Daily	1982-2011	—
	VIC_IGSNRR simulated	0.25°	Daily	1982-2011	Zhang et al. (2014)
Precipitation (P)	Observed, CMA	0.5°	Monthly	1982-2011	—
	TRMM 3B43 V7	0.25°	Monthly	2000-2011	Huffman et al. (2012)
	IGSNRR forcing	0.25°	Daily	1982-2011	Zhang et al. (2014)
Temperature (Temp.)	Observed, CMA	0.5°	Monthly	2000-2011	—
Terrestrial storage change ( $\Delta S$ )	GRACE-CSR	Approx.300-400 km	Monthly	2002-2011	Tapley et al. (2004)
	GRACE-GFZ	Approx.300-400 km	Monthly	2002-2011	Tapley et al. (2004)
	GRACE-JPL	Approx.300-400 km	Monthly	2002-2011	Tapley et al. (2004)
Potential evaporation (PET)	CRU	0.5°	Monthly	1982-2011	Harris et al. (2013)
Actual evaporation (ET)	MTE_E	0.5°	Monthly	1982-2011	Jung et al. (2010)
	VIC_E	0.25°	Daily	1982-2011	Zhang et al. (2014)
	GLEAM_E	0.25°	Daily	1982-2011	Miralles et al. (2011)
	PML_E	0.5°	Monthly	1982-2011	Zhang Y et al. (2016)
	Zhang_E	8 km	Monthly	1983-2006	Zhang et al. (2010)
	GNoah_E	1.0°	3 hourly	1982-2011	Rui (2011)
NDVI	GIMMS NDVI dataset	8 km	15 daily	1982-2011	Tucker et al. (2005)
LAI	GLASS LAI Product	0.05°	8 daily	1982-2011	Liang and Xiao (2012)
Snow Cover	TP Snow composite Products	500 m	Daily	2005-2013	Zhang et al. (2012)
SWE	VIC_IGSNRR simulated	0.25°	Daily	1982-2011	Zhang et al. (2014)
	GlobSnow-2 Product	25 km	Daily	1982-2011	Takala et al. (2011)
Glacier Area	the Second Glacier Inventory Dataset of China	—	—	2005	Guo et al. (2014)

830 **Table 2:** Main features of the 18 TP river basins used in this study. The precipitation and temperature statistics for each basin were calculated from the observed  
831 CMA datasets while the NDVI and LAI statistics were extracted from the GIMMS NDVI dataset and GLASS LAI product. The GA% and SC% represented the  
832 percentages of multiyear-mean glacier cover and snow cover in each basin which were calculated from the Second Glacier Inventory Dataset of China and the daily  
833 TP snow cover dataset (2005-2013)

No.	Station	Altitude (m)	River name	Drainage area (km <sup>2</sup> )	Multiyear-mean (1982-2011) and basin-averaged parameters						
					Q (mm/yr)	Prec. (mm/yr)	Temp.(°C/yr)	NDVI	LAI	GA%	SC%
<b><i>Westerlies-dominated basins:</i></b>											
01	Kulukelangan	2000	Yerqiang	32880.00	158.60	128.34	-5.68	0.05	0.03	10.97	35.03
02	Tongguziluoke	1650	Yulongkashi	14575.00	151.56	134.04	-4.07	0.06	0.04	23.27	35.95
03	Numaitilangan	1880	Keliya	7358.00	103.18	137.14	-4.78	0.06	0.03	10.86	29.16
<b><i>East Asian monsoon-dominated basins:</i></b>											
04	Zelingou	4282	Bayin	5544.00	41.42	340.68	-4.98	0.13	0.09	0.09	21.22
05	Gadatan	3823	Yellow	7893.00	200.95	566.01	-4.60	0.34	0.54	0.13	14.94
06	Xining	3225	Yellow	9022.00	99.90	503.74	0.97	0.36	0.70	0.00	10.06
07	Tongren	3697	Yellow	2832.00	149.36	533.25	-1.37	0.39	0.83	0.00	9.42
08	Tainaihai	2632	Yellow	121972.00	159.48	540.32	-2.40	0.34	0.72	0.09	15.89
09	Huangheyan	4491	Yellow	20930.00	31.18	386.42	-4.81	0.23	0.61	0.00	17.25
10	Jimai	4450	Yellow	45015.00	85.50	441.48	-4.16	0.26	0.52	0.00	20.05
11	Yajiang	2599	Yalong	67514.00	237.66	717.05	-0.23	0.43	0.80	0.15	18.36
12	Zhimenda	3540	Yangtze	137704.00	96.23	405.66	-4.83	0.20	0.26	0.96	17.87
<b><i>Indian monsoon-dominated basins:</i></b>											
13	Jiaoyuqiao	3000	Salween	72844.00	364.26	620.88	-1.89	0.29	0.44	2.02	23.73
14	Pangduo	5015	Brahmaputra	16459.00	348.31	544.59	-1.53	0.27	0.33	1.66	23.33
15	Tangjia	4982	Brahmaputra	20143.00	350.61	555.17	-1.89	0.27	0.34	1.39	21.83
16	Gongbujiangda	4927	Brahmaputra	6417.00	586.96	692.06	-4.24	0.27	0.36	4.12	25.99

17	Nuxia	2910	Brahmaputra	191235.00	307.38	401.35	-0.73	0.22	0.25	1.90	13.50
18	Yangcun	3600	Brahmaputra	152701.00	163.25	349.91	-0.87	0.19	0.18	1.28	10.52

---

834

835

836 **Table 3:** Annual-averaged water storage changes ( $\Delta S$ ) in 18 TP basins derived from GRACE retrievals (2002-2013) from three different processing centers (CSR,  
837 GFZ and JPL)

Basin	Water storage Change ( $\Delta S$ ,mm)		
	CSR	GFZ	JPL
<b><i>Westerlies-dominated basins:</i></b>			
Kulukelangan	-0.16	-0.16	-0.00
Tongguziluoke	0.10	0.10	0.28
Numaitilangan	0.24	0.22	0.41
<b><i>East Asian monsoon-dominated basins:</i></b>			
Zelingou	0.63	0.41	0.69
Gadatan	0.02	-0.24	-0.03
Xining	-0.08	-0.35	-0.14
Tongren	-0.13	-0.41	-0.21
Tainaihai	0.12	-0.16	0.10
Huangheyan	0.60	0.35	0.70
Jimai	0.41	0.15	0.48
Yajiang	-0.23	-0.50	-0.21
Zhimenda	0.57	0.38	0.78
<b><i>Indian monsoon-dominated basins:</i></b>			
Jiaoyuqiao	-1.00	-1.13	-0.79
Nuxia	-1.42	-1.44	-1.31
Pangduo	-1.21	-1.29	-1.02
Tangjia	-1.40	-1.46	-1.24
Gongbujiangda	-1.61	-1.67	-1.47
Yangcun	-1.33	-1.34	-1.21

838 **Table 4:** Nonparametric trends for different ET estimates during the period 1982-2006 detected by modified Mann-Kendall test, the bold number showed the  
 839 detected trend is statistically significant at the 0.05 level

840	Basin	ET <sub>wb</sub>	GLEAM_E	VIC_E	Zhang_E	PML_E	MET_E	GNoah_E
842	<i>Westerlies-dominated basins:</i>							
	Kulukelangan	<b>-0.09</b>	0.09	<b>0.18</b>	–	0.03	-0.01	0.07
843	Tongguziluoke	-0.02	0.10	<b>0.13</b>	–	0.03	<b>-0.08</b>	0.19
	Numaitilangan	0.04	<b>0.10</b>	0.14	–	0.14	<b>-0.10</b>	0.22
844	<i>East Asian monsoon-dominated basins:</i>							
	Zelingou	<b>0.13</b>	<b>0.23</b>	0.11	<b>0.09</b>	0.04	<b>0.06</b>	0.02
845	Gadatan	-0.09	0.25	0.070	-0.10	-0.01	<b>0.06</b>	-0.07
	Xining	-0.06	<b>0.54</b>	0.01	-0.08	0.01	0.02	-0.06
846	Tongren	-0.06	<b>0.34</b>	-0.15	<b>-0.17</b>	0.07	0.02	0.13
	Tainaihai	0.06	<b>0.28</b>	-0.03	<b>-0.11</b>	0.04	<b>0.05</b>	0.04
847	Huangheyang	0.08	<b>0.19</b>	-0.01	<b>-0.10</b>	<b>0.08</b>	<b>0.05</b>	<b>0.10</b>
	Jimai	-0.07	<b>0.23</b>	-0.01	-0.08	0.03	<b>0.05</b>	0.10
848	Yajiang	0.17	<b>0.26</b>	<b>0.06</b>	<b>-0.21</b>	-0.01	0.03	-0.02
	Zhimenda	0.11	<b>0.28</b>	0.10	0.01	0.07	<b>0.04</b>	0.07
849	<i>Indian monsoon-dominated basins:</i>							
	Jiaoyuqiao	<b>0.18</b>	<b>0.28</b>	0.10	<b>-0.11</b>	0.05	<b>0.05</b>	0.07
850	Nuxia	<b>-0.09</b>	<b>0.25</b>	0.09	<b>-0.10</b>	<b>0.12</b>	<b>0.04</b>	0.10
	Pangduo	0.05	<b>0.28</b>	<b>0.17</b>	<b>-0.07</b>	0.07	<b>0.07</b>	<b>0.11</b>
851	Tangjia	0.09	<b>0.26</b>	<b>0.17</b>	<b>-0.09</b>	<b>0.20</b>	<b>0.06</b>	<b>0.12</b>
	Gongbujiangda	-0.26	0.12	0.13	<b>-0.16</b>	<b>0.19</b>	0.01	<b>0.15</b>
852	Yangcun	0.03	<b>0.28</b>	0.08	<b>-0.06</b>	0.10	0.04	0.09

853 **Figure captions:**

854 **Figure1.** Map of river basins and hydrological gauging stations (green dots) over the  
855 Tibetan Plateau (TP) used in this study. The grey shading shows the topography of TP  
856 in meters above the sea level and the blue shading exhibits the glaciers distribution in  
857 TP extracted from the Second Glacier Inventory Dataset of China.

858 **Figure 2.** Comparison of VIC\_IGSNRR simulated and observed monthly runoff for  
859 Tangnaihai and Panduo stations (a and b) as well as (c) basin-averaged monthly  
860 TRMM, CMA gridded and IGSNRR forcing precipitations for the smallest basin  
861 (Tongren station) over the period 1982-2011. (d) shows the comparison of TRMM  
862 (blue) and IGSNRR forcing (red) precipitations against CMA gridded precipitation for  
863 18 river basins over TP during the period 2000-2011.

864 **Figure 3.** Comparison of different ET products against the calculated ET through the  
865 water balance method ( $ET_{wb}$ ) at the monthly time scale for 18 TP basins during the  
866 period 1983-2006. The boxplot of monthly estimates of different ET products for 18  
867 TP basins are shown in (a) while the correlation coefficients and  
868 root-mean-square-errors (RMSEs, mm/month) for each ET product relatively to  $ET_{wb}$   
869 are exhibited in (b).

870 **Figure 4.** General water and energy status (a. the perspective of Budyko framework)  
871 and their relationships with glacier (b) and vegetation (c and d) for eighteen TP river  
872 basins (1983-2006). The ET used in this figure is calculated from the bias-corrected  
873 water balance method.

874 **Figure 5.** Seasonal cycles (1982-2011) of water budget components in westerlies-  
875 dominated (column 1), East Asian monsoon-dominated (columns 2-4) and Indian  
876 monsoon-dominated (columns 5-6) TP basins.

877 **Figure 6.** Seasonal cycles (1982-2011) of air temperature and vegetation parameters  
878 in westerlies-dominated (column 1), East Asian monsoon-dominated (columns 2-4)  
879 and Indian monsoon-dominated (columns 5-6) TP basins.

880 **Figure 7.** Seasonal cycles (1982-2011) of snow cover and snow water equivalent  
881 (SWE) in westerlies-dominated (column 1), East Asian monsoon-dominated (columns

882 2-4) and Indian monsoon-dominated (columns 5-6) TP basins. The snow cover was  
883 extracted from cloud free snow composite product during the period 2005-2013. It  
884 should also be noted that the GlobSnow data are not available for some basins.

885 **Figure 8.** Sen's slopes of water budget components and vegetation parameters in  
886 westerlies-dominated TP basins during the period of 1982-2011. To clearly exhibit the  
887 nonparametric trends of all variables in one panel, the Sen's Slopes of Q, P,  $ET_{wb}$  and  
888 PET have been multiplied by 1/12 (unit: mm/month). The double red stars showed  
889 that the trend was statistically significant at the 0.05 level.

890 **Figure 9.** Linear and non-parametric trends of westerly, Indian monsoon and East  
891 Asian summer monsoon during the period 1982-2011 revealed prospectively by the  
892 Asian Zonal Circulation Index, Indian Ocean Dipole Mode Index and East Asian  
893 Summer Monsoon Index.

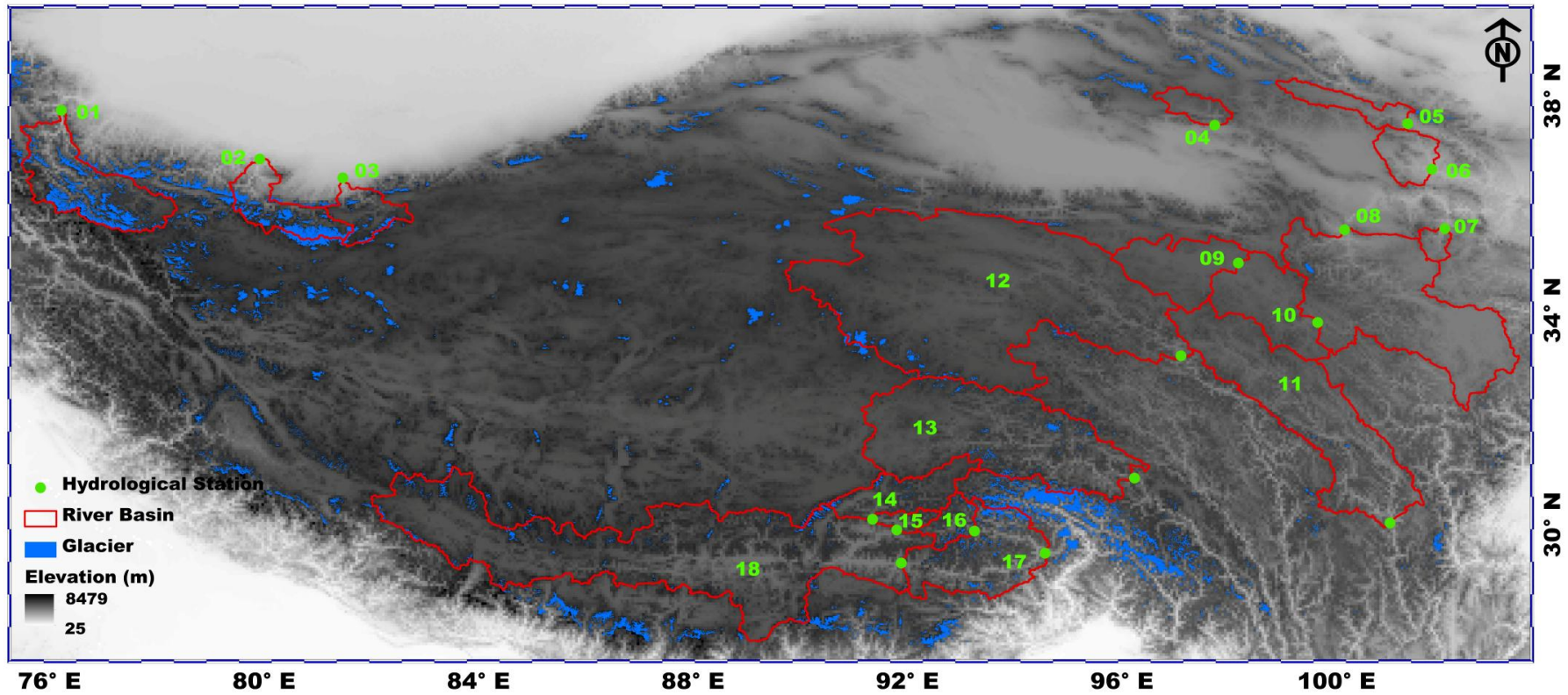
894 **Figure 10.** Similar to Figure 8 but for East Asian monsoon-dominated TP basins. It  
895 should be noted that the GlobSnow data are not available for some basins. The double  
896 red stars showed that the trend was statistically significant at the 0.05 level.

897 **Figure 11.** Similar to Figure 8 but for Indian monsoon-dominated TP basins. It should  
898 be noted that the GlobSnow data are not available for some basins. The double red  
899 stars showed that the trend was statistically significant at the 0.05 level.

900 **Figure 12.** Uncertainties in seasonal cycles of  $ET_{wb}$  calculated from three precipitation  
901 products (CMA gridded, IGSNRR\_Forcing and TRMM precipitation) in 18 TP basins.  
902 The comparisons were conducted during the period 2000-2011 when TRMM data was  
903 available.

904 **Figure 13.** Uncertainties in annual trends of  $ET_{wb}$  (b) calculated from two precipitation  
905 products (CMA gridded and IGSNRR\_Forcing) (a) in 18 TP basins. The comparisons  
906 were conducted during the period 1982-2011 (TRMM data was not available for the  
907 whole period).

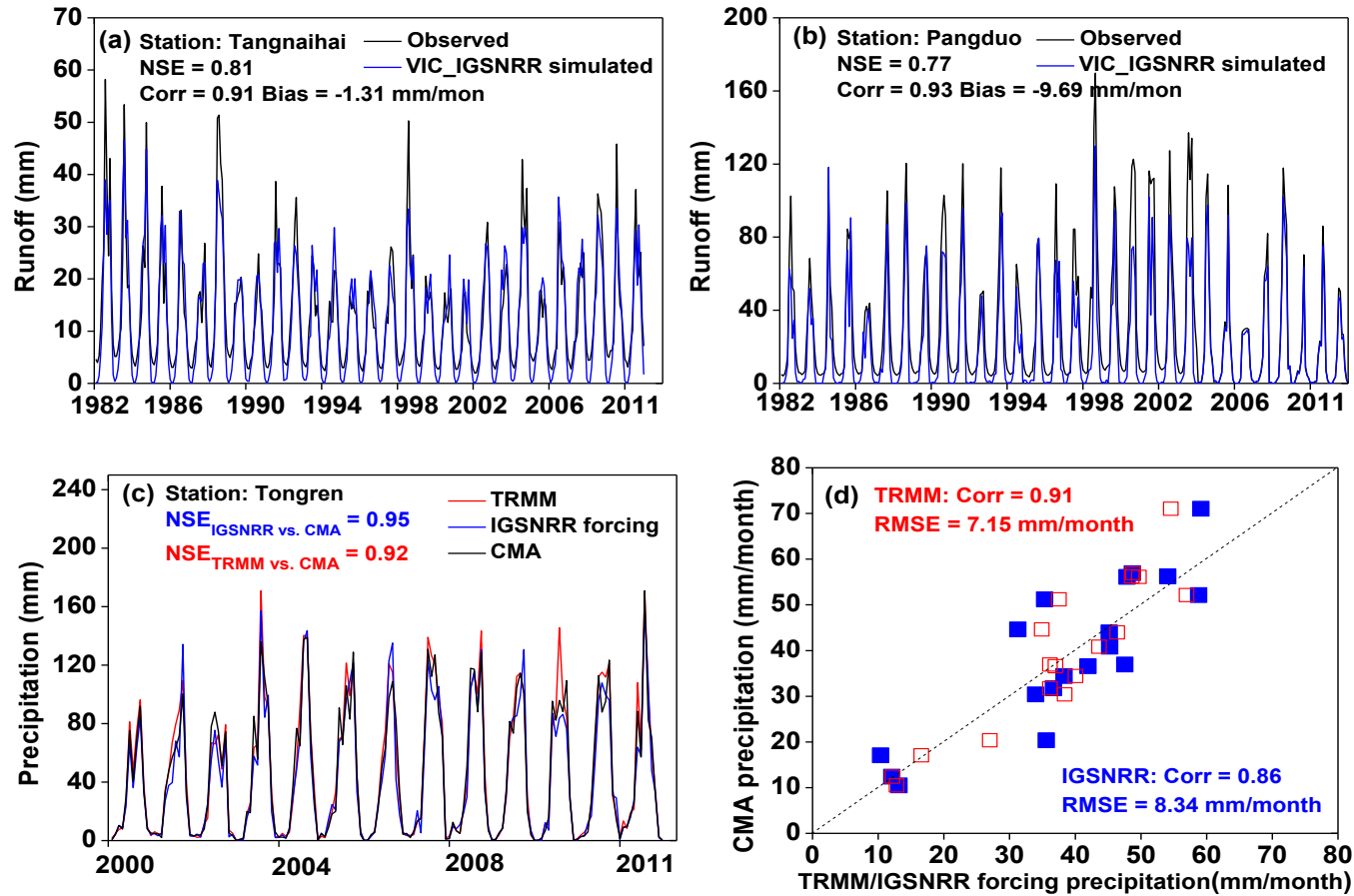
908 **Figure 1.** Map of river basins and hydrological gauging stations (green dots) over the Tibetan Plateau (TP) used in this study. The grey shading shows the  
909 topography of TP in meters above the sea level and the blue shading exhibits the glaciers distribution in TP extracted from the Second Glacier Inventory Dataset of  
910 China.



911  
912



913 **Figure 2.** Comparison of VIC\_IGSNRR simulated and observed monthly runoff for Tangnaihai and Panduo stations (a and b) as well as (c) basin-averaged  
 914 monthly TRMM, CMA gridded and IGSNRR forcing precipitations for the smallest basin (Tongren station) over the period 1982-2011. (d) shows the comparison of  
 915 TRMM (blue) and IGSNRR forcing (red) precipitations against CMA gridded precipitation for 18 river basins over TP during the period 2000-2011.

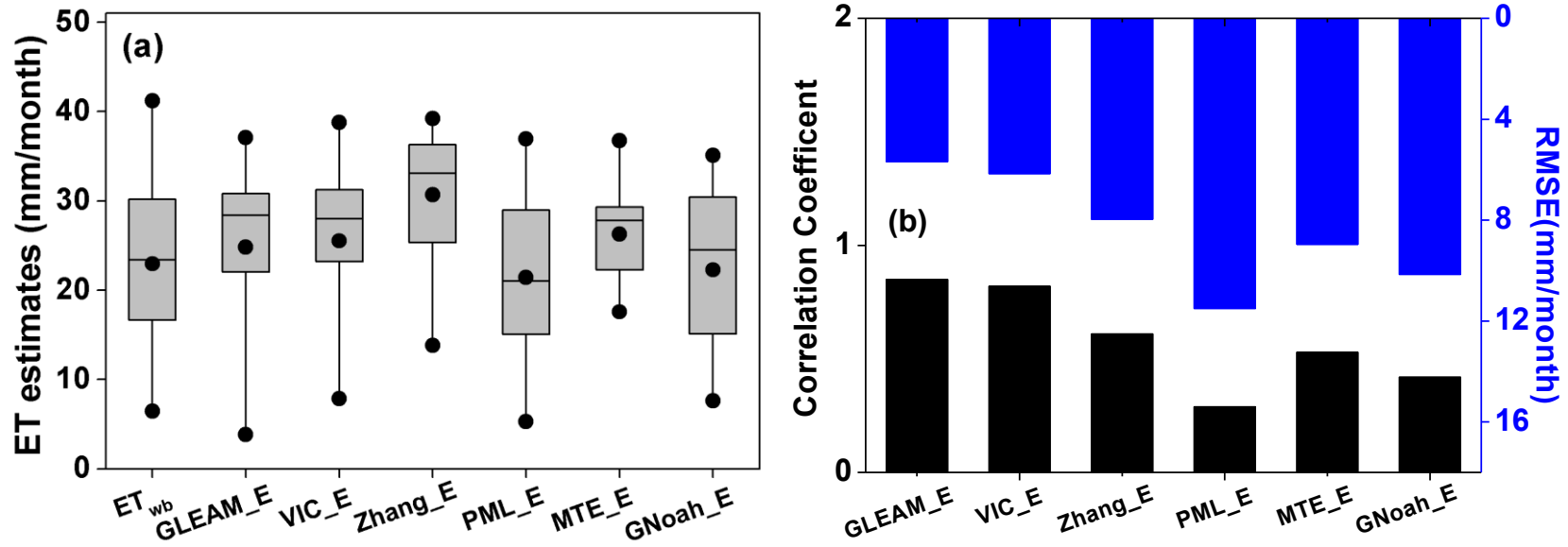


916

917

918

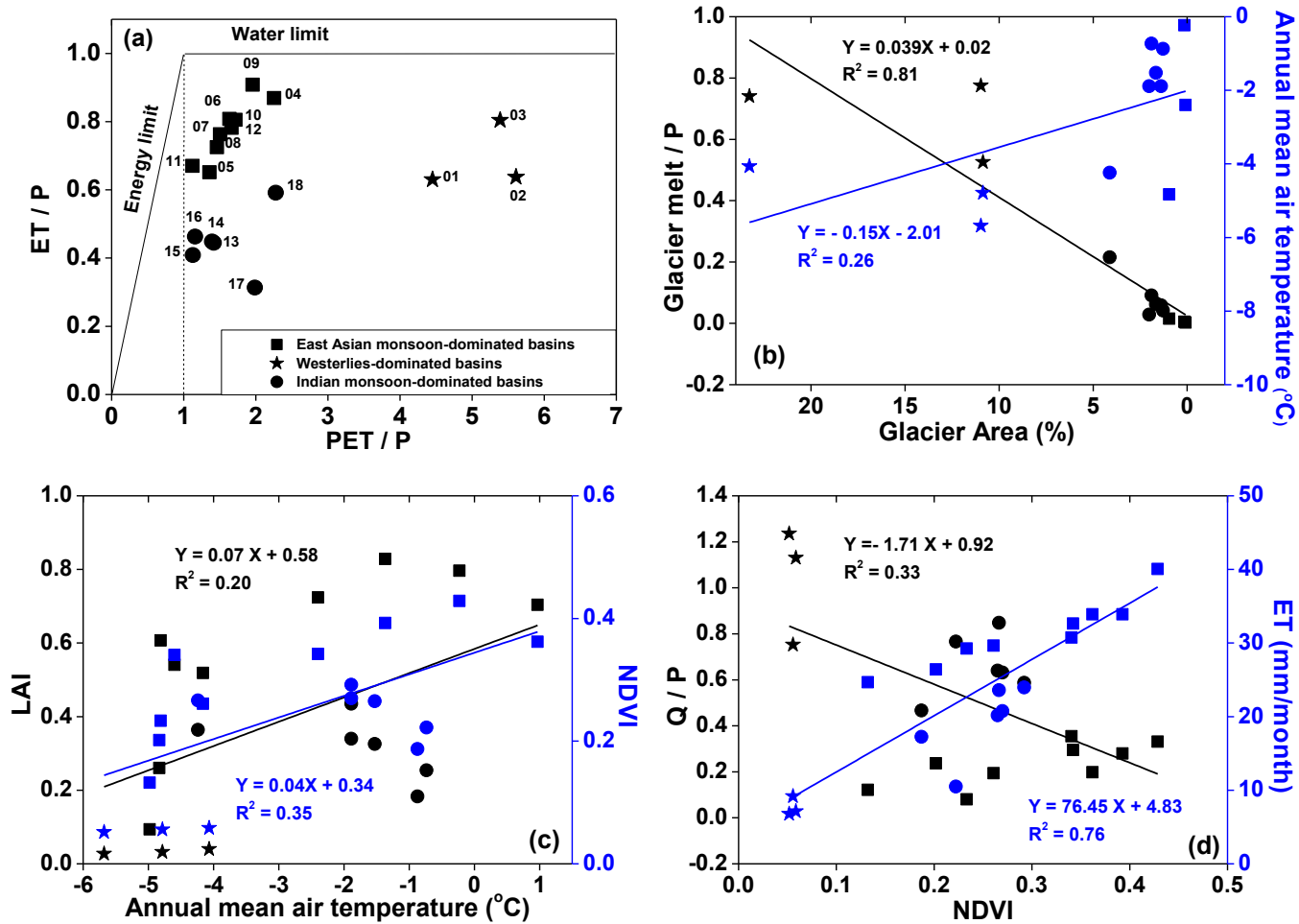
919 **Figure 3.** Comparison of different ET products against the calculated ET through the water balance ( $ET_{wb}$ ) at the monthly time scale for 18 river basins over the  
 920 Tibetan Plateau during the period 1983-2006. The boxplot of monthly estimates of different ET products for 18 TP basins are shown in (a) while the correlation  
 921 coefficients and root-mean-square-errors (RMSEs, mm/month) for each ET product relatively to  $ET_{wb}$  are exhibited in (b).



922

923

924 **Figure 4.** General water and energy status (a. the perspective of Budyko framework) and their relationships with glacier (b) and vegetation (c and d) for eighteen  
 925 TP river basins (1983-2006). The ET used in this figure is calculated from the bias-corrected water balance method.

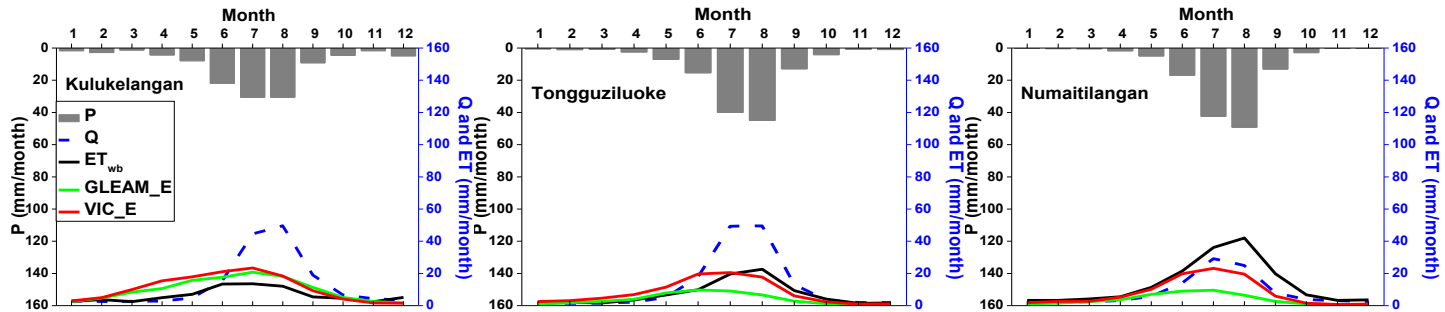


926

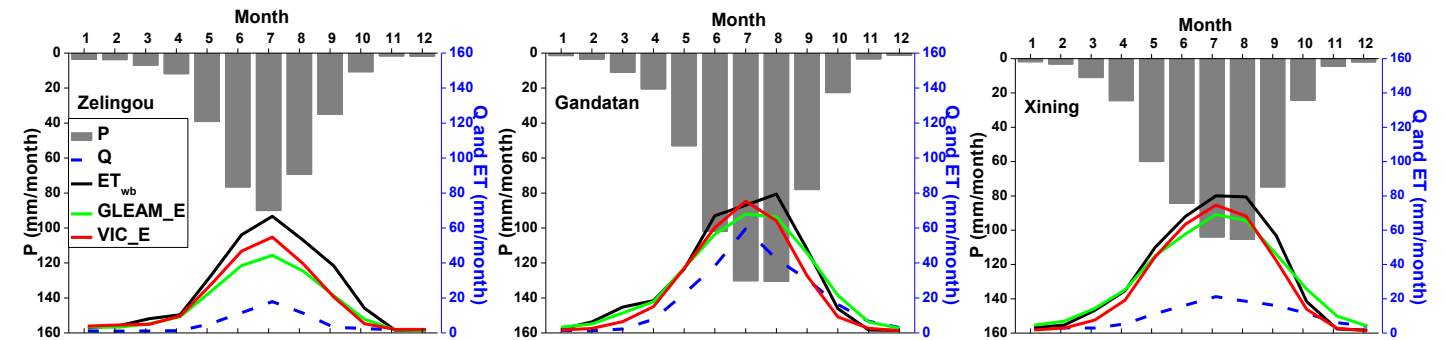
927

928 **Figure 5.** Seasonal cycles (1982-2011) of water budget components in westerlies-dominated (column 1), East Asian monsoon-dominated (columns 2-4) and Indian  
 929 monsoon-dominated (columns 5-6) TP basins.

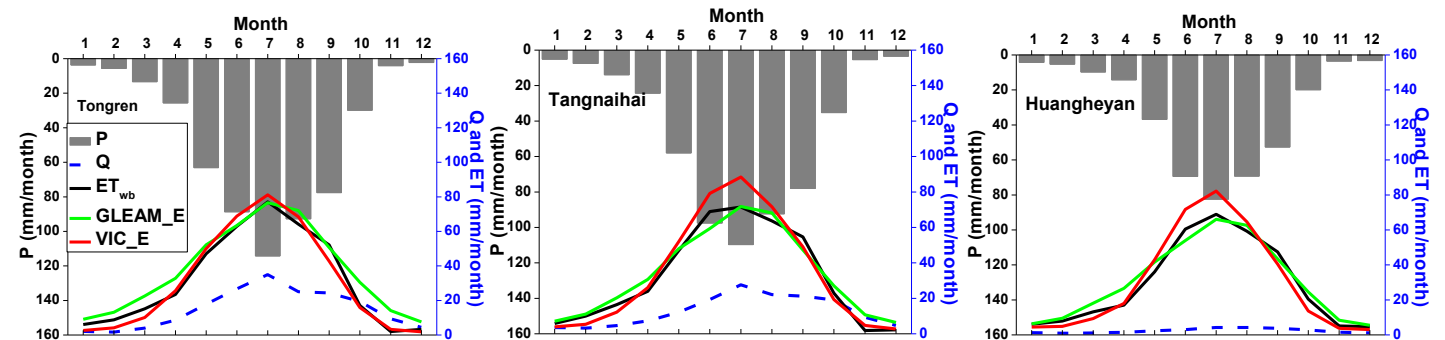
930



931

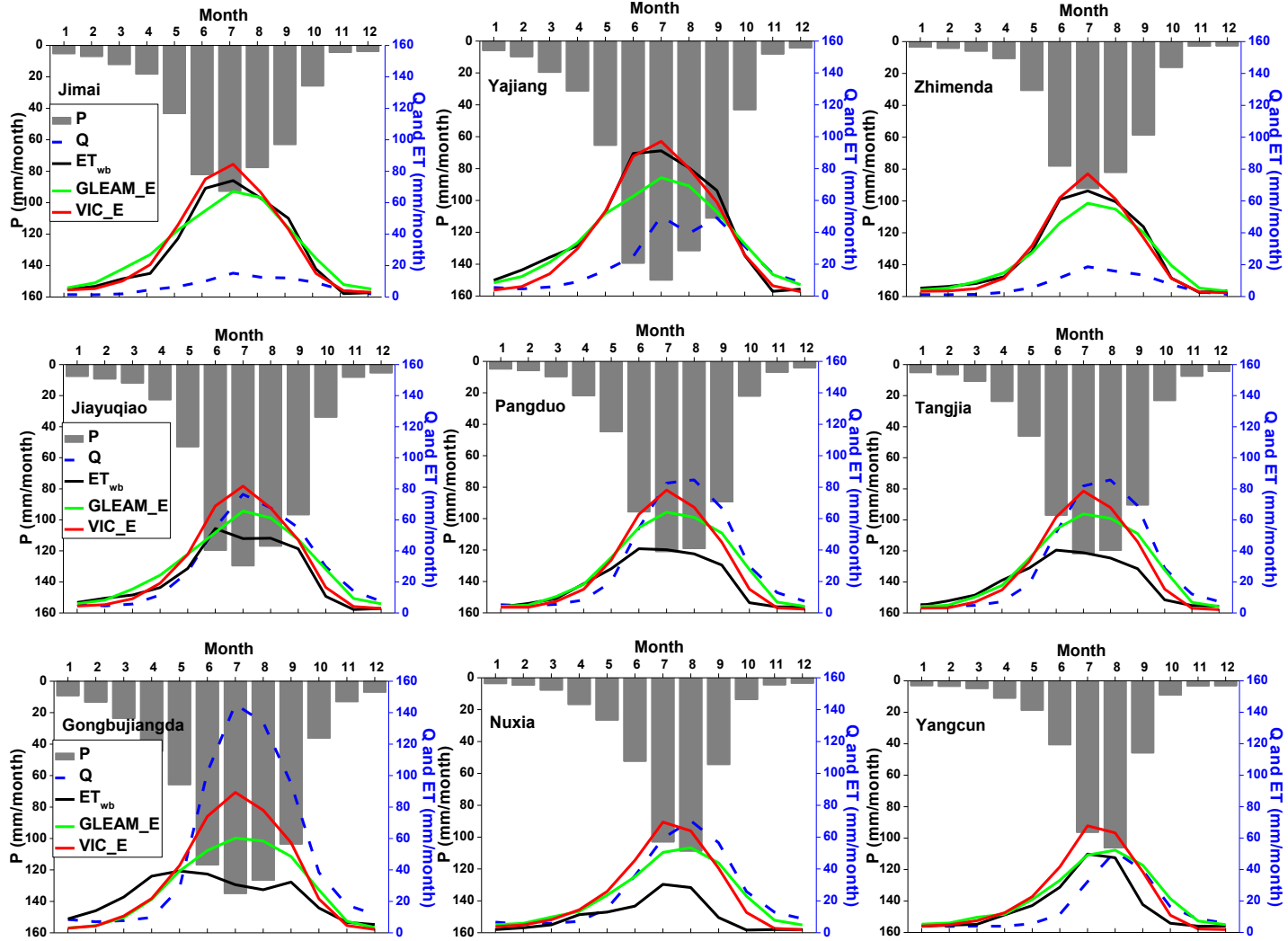


932



933

Figure 5: (continued)

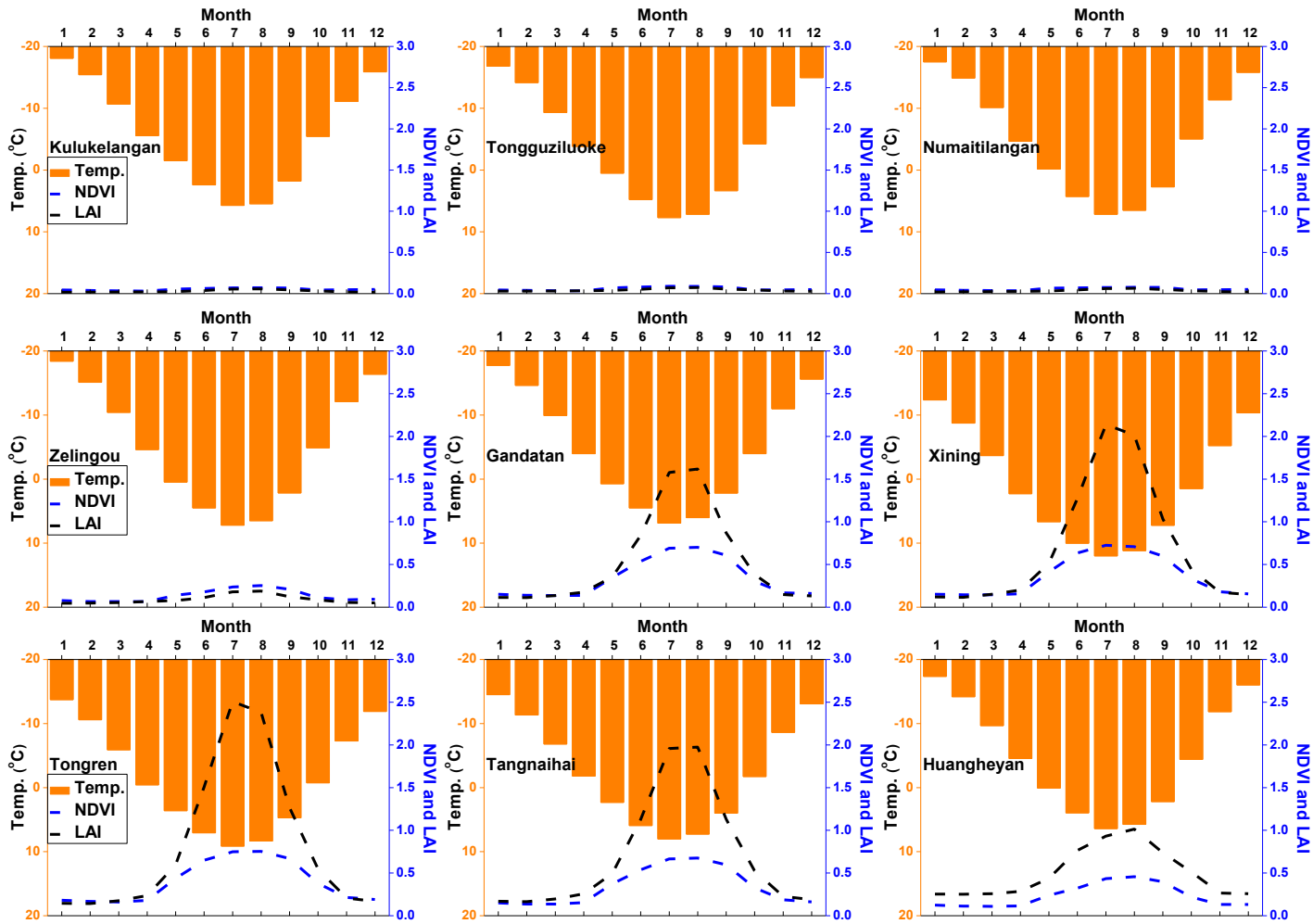


934

935

936

937 **Figure 6.** Seasonal cycles (1982-2011) of air temperature and vegetation parameters in westerlies-dominated (column 1), East Asian monsoon-dominated (columns  
 938 2-4) and Indian monsoon-dominated (columns 5-6) TP basins.



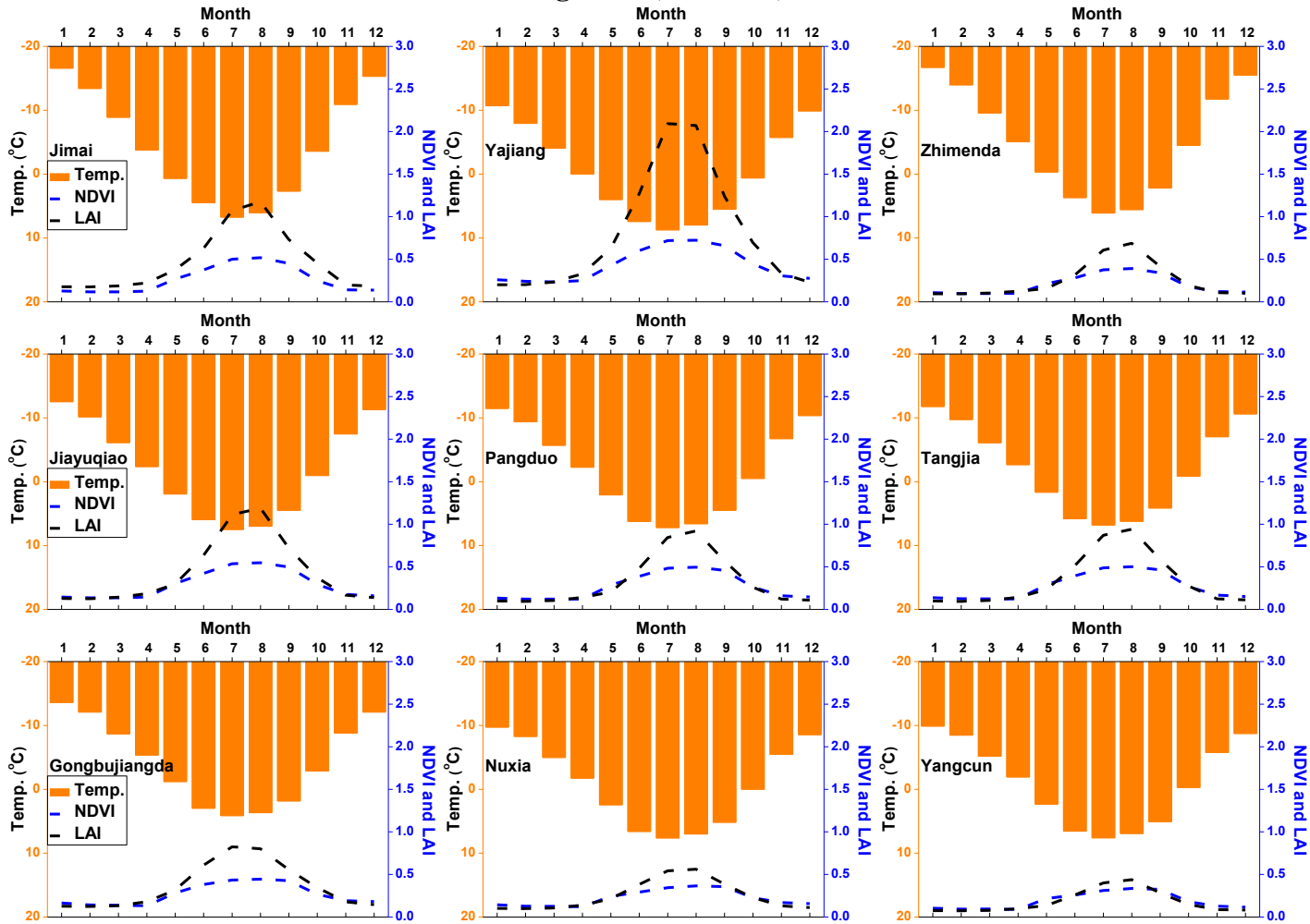
939

940

941

942

Figure 6: (continued)



943

944

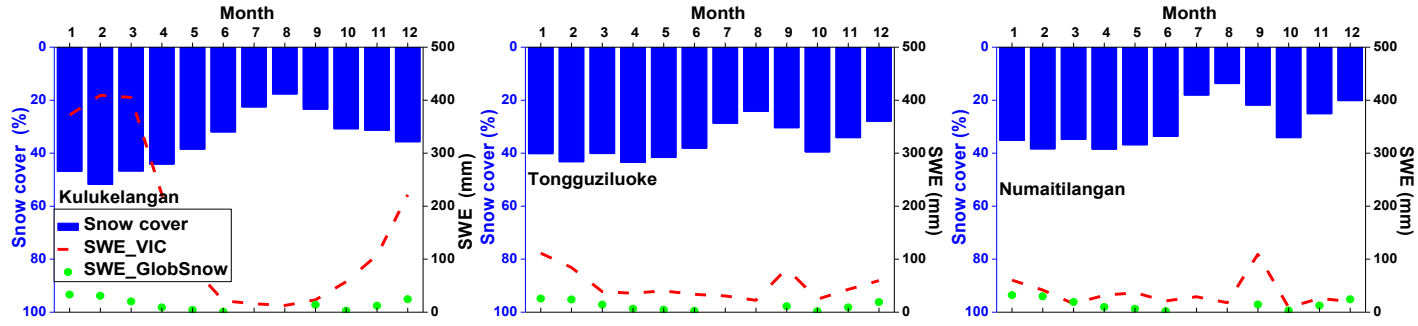
945

946

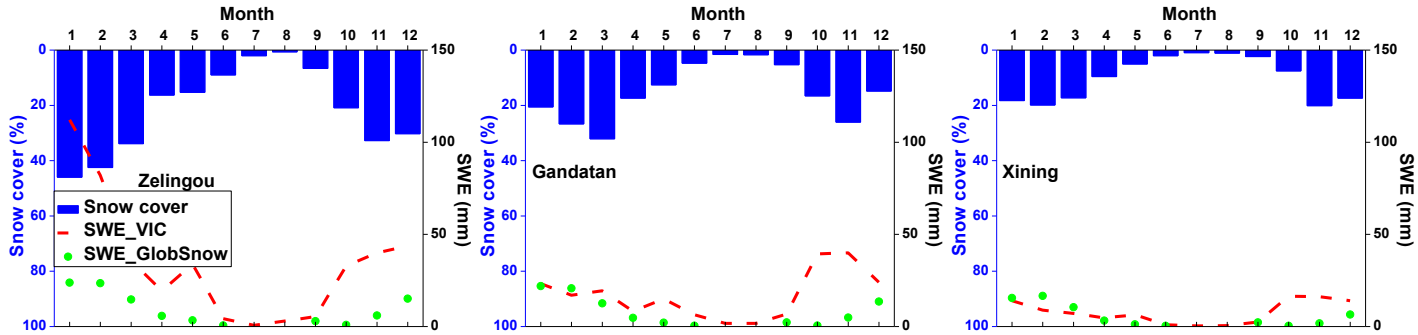
947 **Figure 7.** Seasonal cycles (1982-2011) of snow cover and snow water equivalent (SWE) in westerlies-dominated (column 1), East Asian monsoon- dominated  
948 (columns 2-4) and Indian monsoon-dominated (columns 5-6) TP basins. The snow cover was extracted from cloud free snow composite product during the period  
949 2005-2013. It should also be noted that the GlobSnow data are not available for some basins.  
950



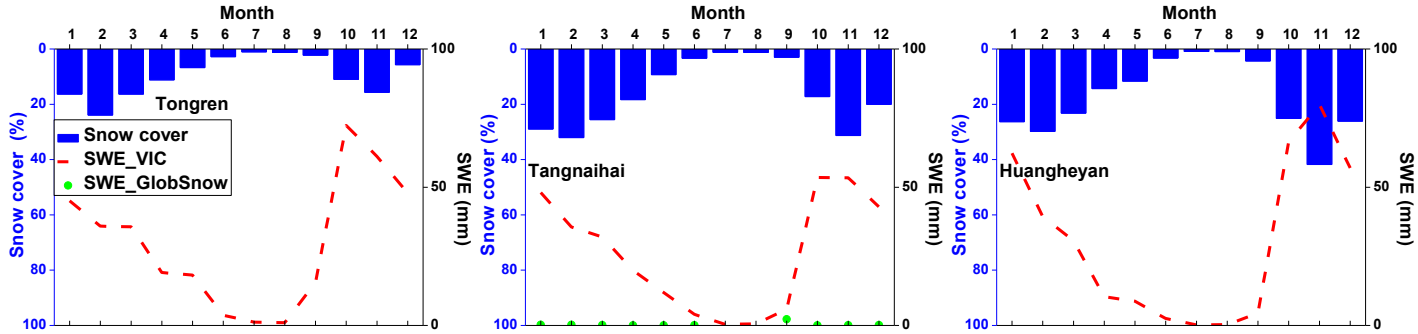
951



952



953

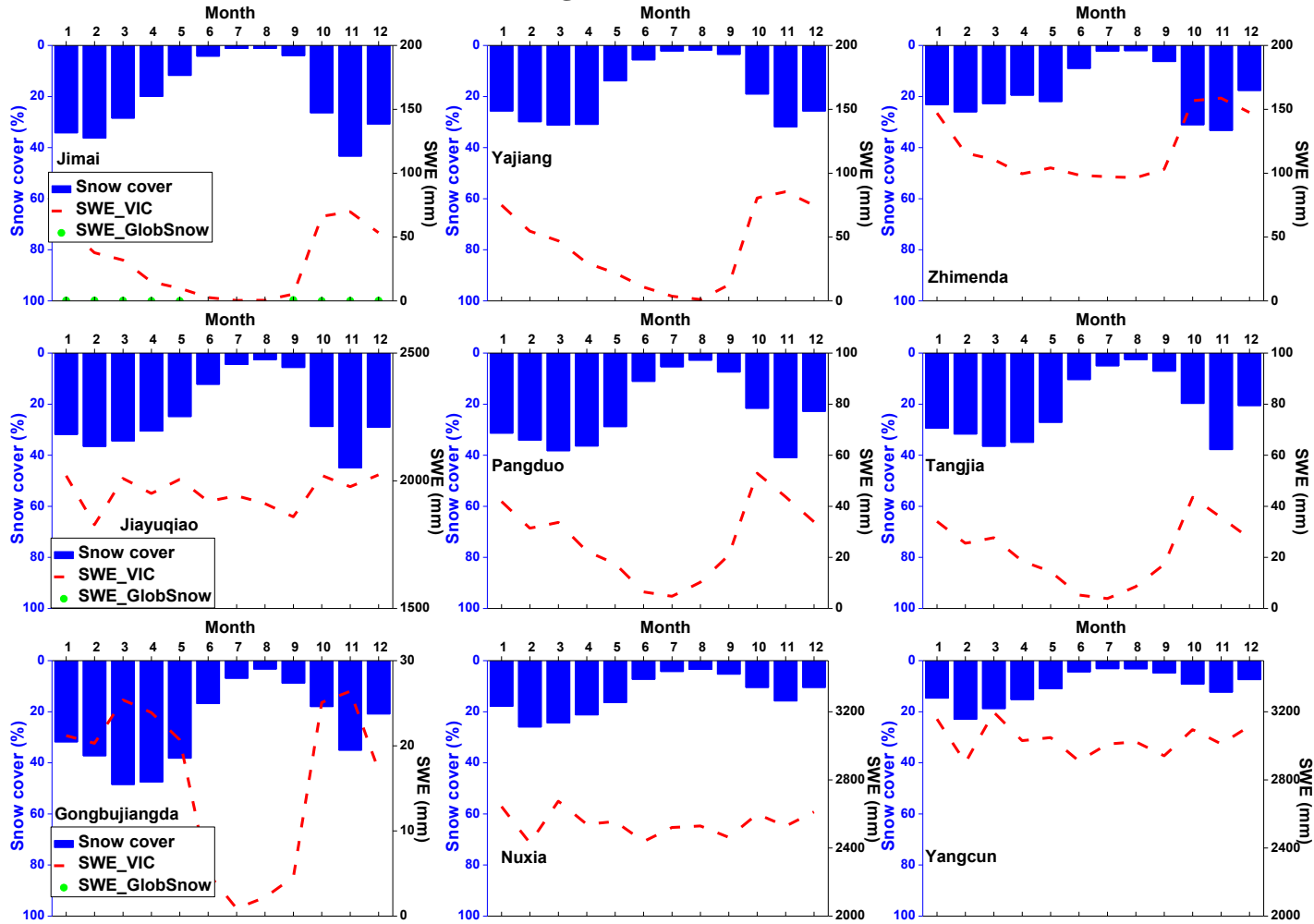


954

955

956

Figure 7: (continued)



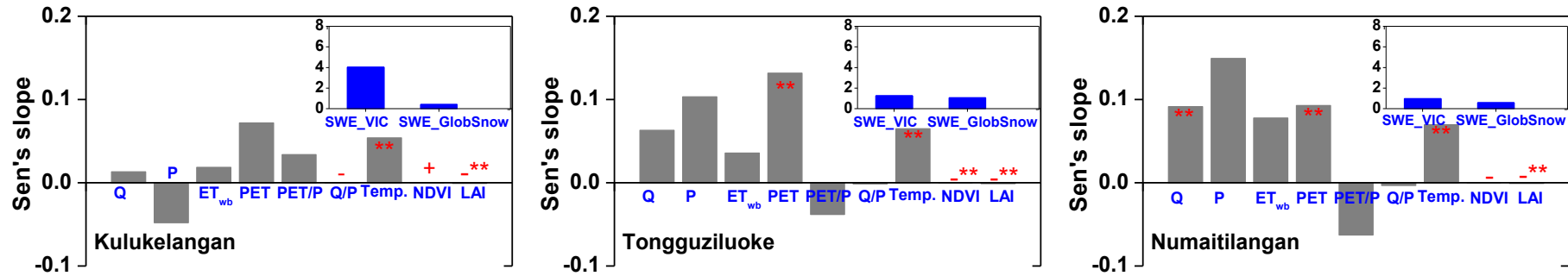
957

958

959

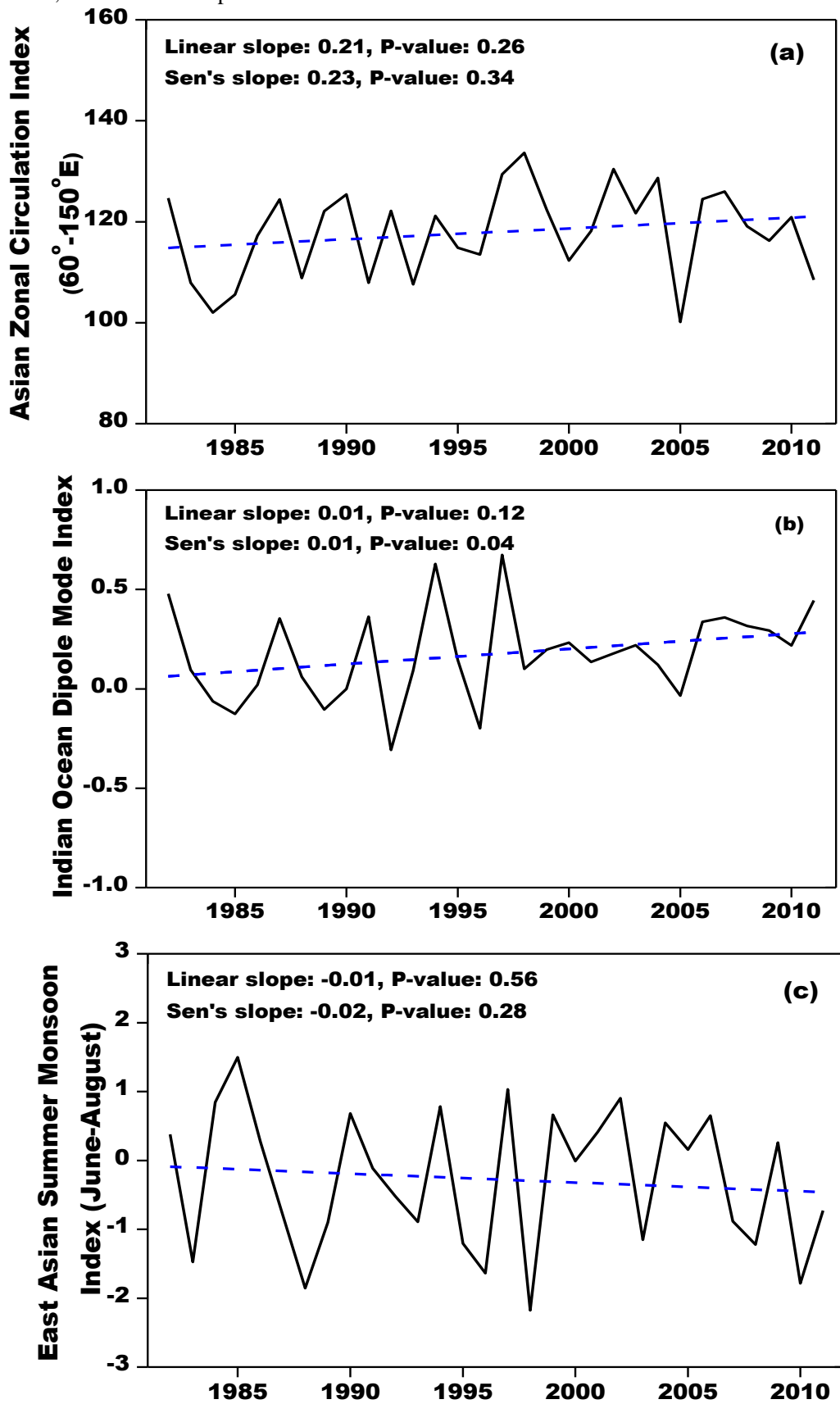
960

961 **Figure 8.** Sen's slopes of water budget components and vegetation parameters in westerlies-dominated TP basins during the period of 1982-2011. To clearly  
 962 exhibit the nonparametric trends of all variables in one panel, the Sen's Slopes of Q, P, ET<sub>wb</sub> and PET have been multiplied by 1/12 (unit: mm/month). The double  
 963 red stars showed that the trend was statistically significant at the 0.05 level.



964  
965

966 **Figure 9.** Linear and non-parametric trends of westerly, Indian monsoon and East Asian summer  
 967 monsoon during the period 1982-2011 revealed prospectively by the Asian Zonal Circulation  
 968 Index, Indian Ocean Dipole Mode Index and East Asian Summer Monsoon Index.



969

970

971

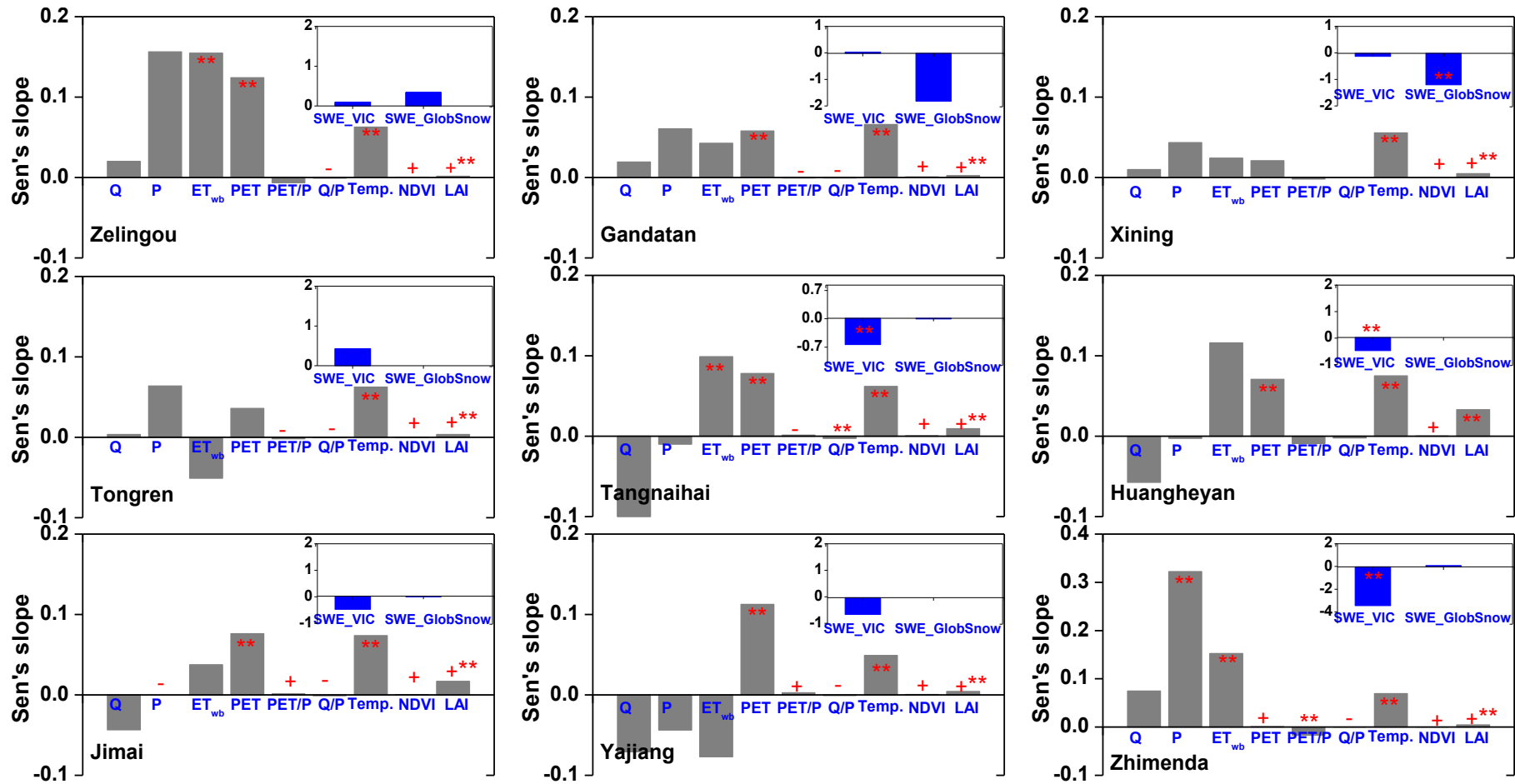
972  
973

**Figure 10.** Similar to Figure 8 but for East Asian monsoon-dominated TP basins. It should be noted that the GlobSnow data are not available for some basins.

974

975

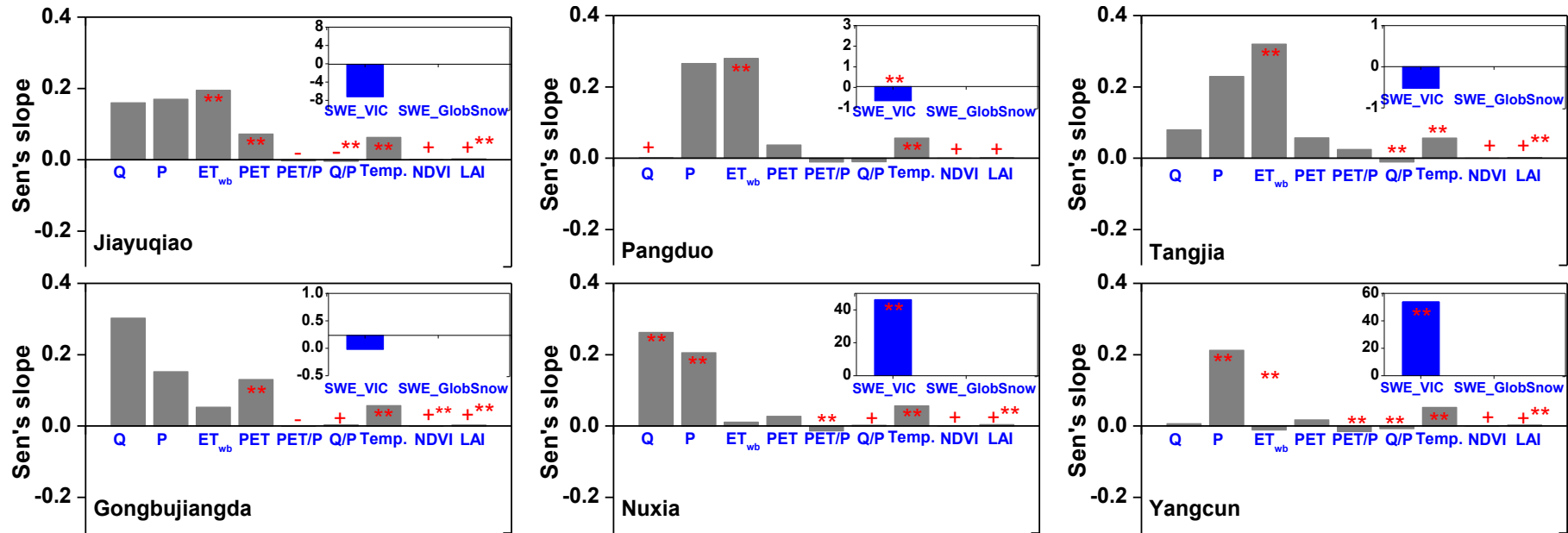
976  
977  
978



979  
980

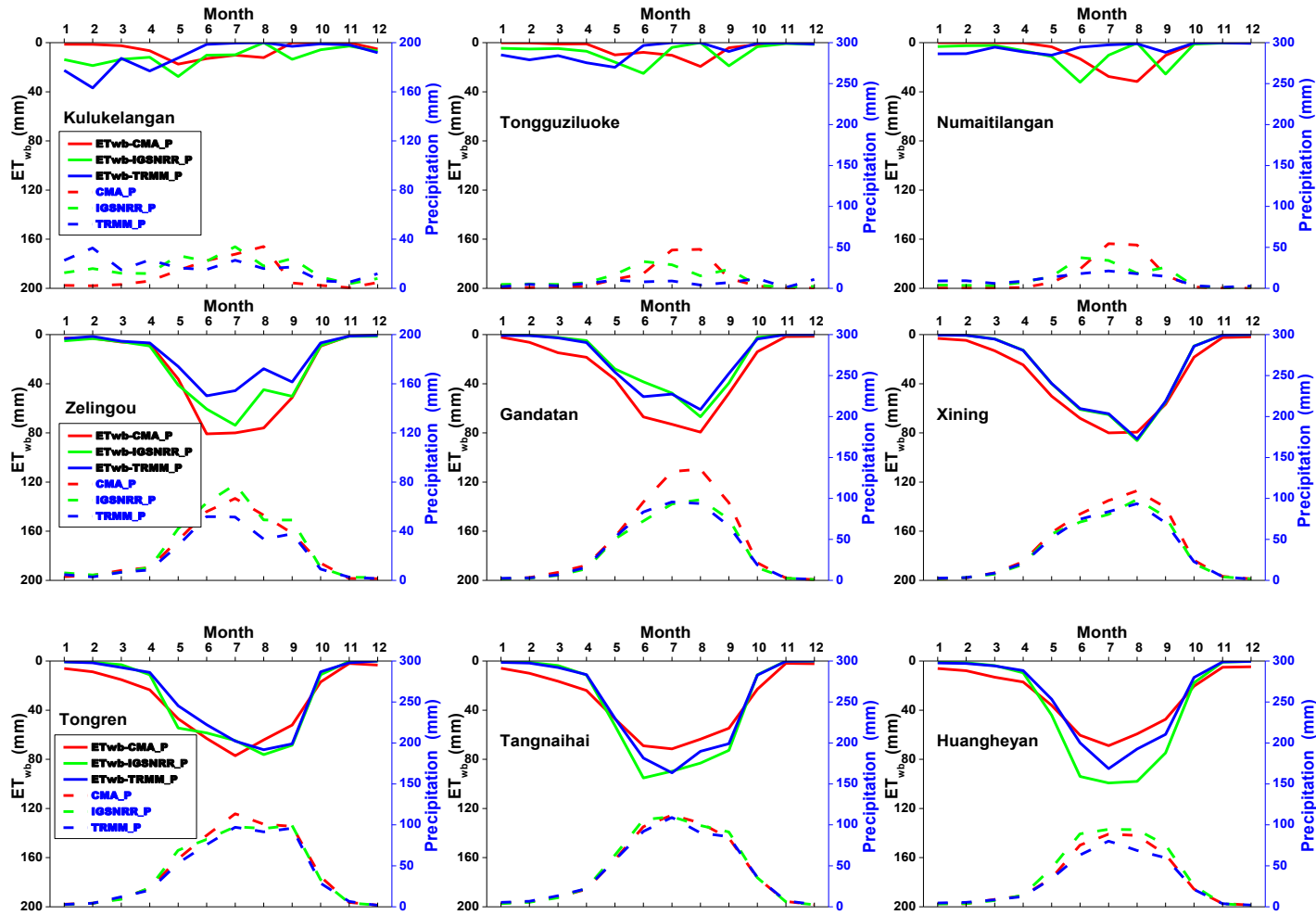
**Figure 11.** Similar to Figure 8 but for Indian monsoon-dominated TP basins. It should be noted that the GlobSnow data are not available for some basins.

981



982  
983

984 **Figure 12.** Uncertainties in seasonal cycles of  $ET_{wb}$  calculated from three precipitation products (CMA gridded, IGSNRR\_Forcing and TRMM precipitation) in 18 TP  
 985 basins. The comparisons were conducted during the period 2000-2011 when TRMM data was available.



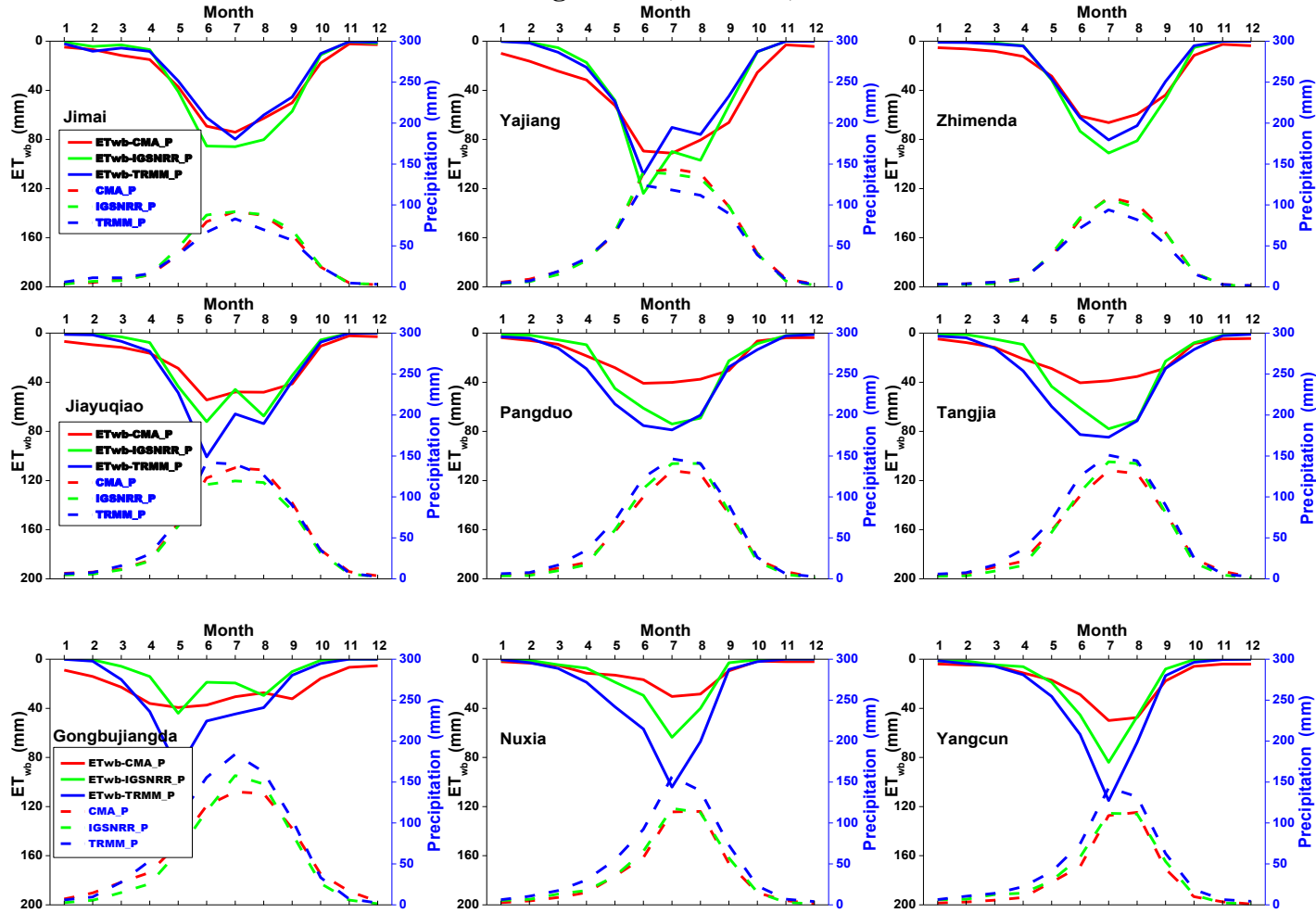
986

987  
 988

989

990

Figure 12: (continued)



991

992

993

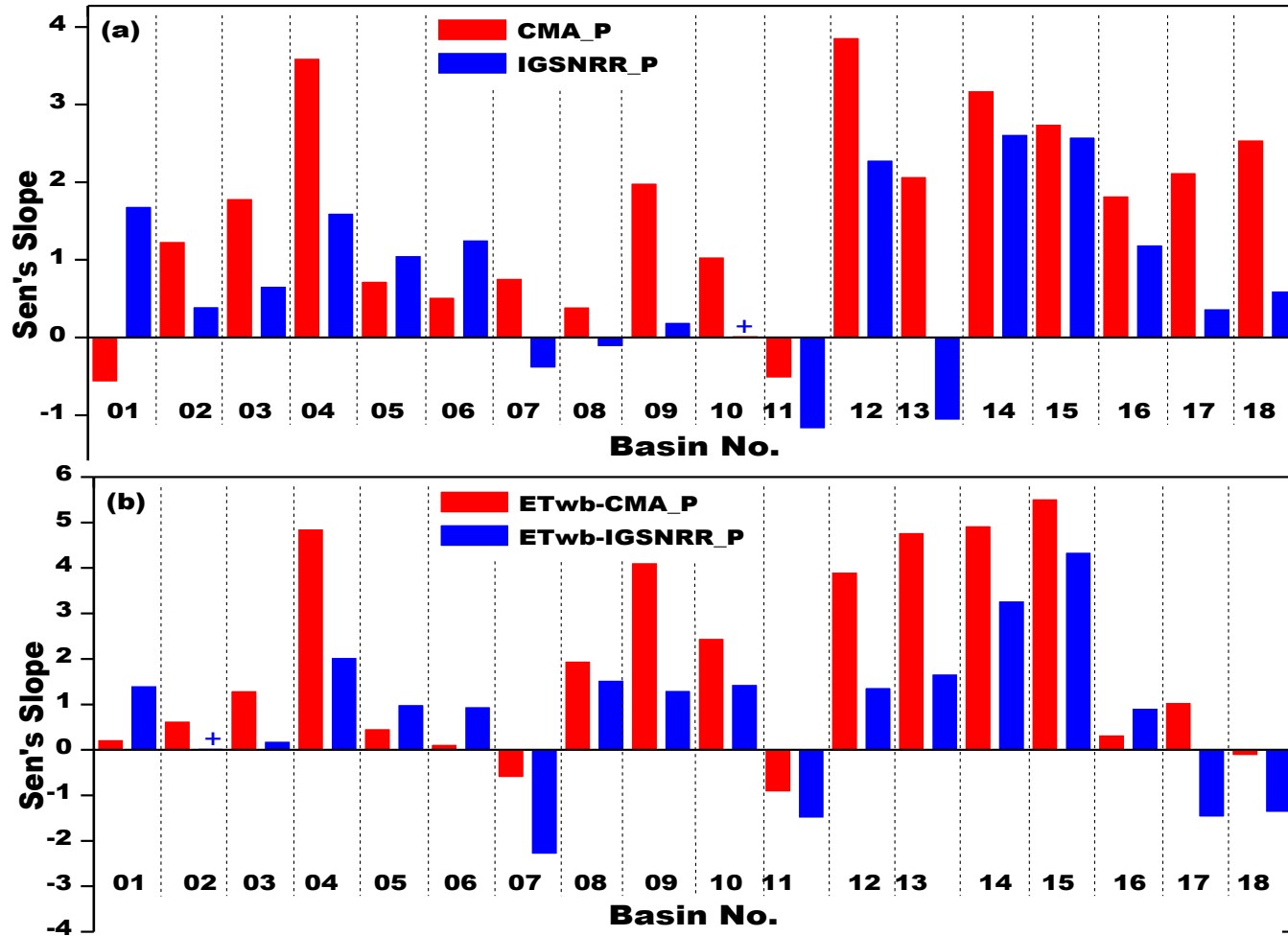
994

995

996



997 **Figure 13.** Uncertainties in annual trends of  $ET_{wb}$  (b) calculated from two precipitation products (CMA gridded and IGSNRR\_Forcing) (a) in 18 TP basins. The  
 998 comparisons were conducted during the period 1982-2011 (TRMM data was not available for the whole period).



999

1000